| AD NUMBER |
|---|
| AD102193 |

| CLASSIFICATION CHANGES | |
|---|---|
| TO: | UNCLASSIFIED |
| FROM: | CONFIDENTIAL |

| LIMITATION CHANGES |
|---|

TO:

Approved for public release; distribution is unlimited.

FROM:

Distribution authorized to U.S. Gov't. agencies and their contractors; Administrative/Operational Use; 15 MAY 1956. Other requests shall be referred to Office of Naval Research, 875 N. Randolph St., Arlington, VA 22203.

AUTHORITY

ONR ltr 28 Jul 1977 ; ONR ltr 28 Jul 1977

THIS REPORT HAS BEEN DELIMITED
AND CLEARED FOR PUBLIC RELEASE
UNDER DOD DIRECTIVE 5200.20 AND
NO RESTRICTIONS ARE IMPOSED UPON
ITS USE AND DISCLOSURE.

DISTRIBUTION STATEMENT A

APPROVED FOR PUBLIC RELEASE;
DISTRIBUTION UNLIMITED.

Contract No. Nonr-1675(00)

# DUCTED PROPELLER
# ASSAULT TRANSPORT

Stability and Control

Report No. D181-945-005

15 May 1956

BELL *Aircraft* CORP.

# BELL *Aircraft* CORPORATION
BUFFALO 5.                                    NEW YORK

# TECHNICAL DATA

### NOTICE

This document contains information affecting the national defense of the United States within the meaning of the Espionage Laws, Title 18, U.S.C., Sections 793 and 794. The transmission or the revelation of its contents in any manner to an unauthorized person is prohibited by law.

BY ~~S. D. Vollo, L. Brassaw~~ DATE . . May 15, 1956

CHECKED . . . . . . . . . . . . DATE . . . . . . . . . . . .

APPROVED ~~J. O'Malley~~, Project Aerodynamicist DATE . . May 15, 1956

APPROVED ~~P. C. Emmons~~, Chief Aerodynamicist DATE . . May 15, 1956

CONTRACT NO.   Nonr 1675 (00)                    NO. OF PAGES   96

| REPORT NO. D181-945-005 | MODEL |
|---|---|
| STABILITY AND CONTROL | |
| COPY NO. | |

**REVISIONS**

| DATE | PAGE NO. | |
|---|---|---|
| | | |

Form E9-1 C

### FORWARD

Contract Nonr-1675(00) was awarded to Bell Aircraft Corporation by the Office of Naval Research under sponsorship of the Army Transportation Corps. This is one of a series of five study contracts let to investigate the application of various schemes to the design of Vertical Take-off and Landing (VTOL) or Short Take-off (STO) Assault Transport Aircraft.

The particular field of investigation at Bell Aircraft is the application of ducted propeller propulsion systems to the design of aircraft capable of performing the Assault Transport mission. The results of the investigation are presented in the following listed reports:

| TITLE | REPORT NUMBER |
|---|---|
| Summary Report | D181-945-001 |
| Design Report | D181-945-002 |
| Survey of the State of the Art | D181-945-003 |
| Performance | D181-945-004 |
| Stability and Control | D181-945-005 |
| Duct and Propeller Analysis | D181-945-006 |
| Preliminary Structural Analysis | D181-945-007 |

## TABLE OF CONTENTS

## LIST OF FIGURES

## LIST OF FIGURES (Cont)

## LIST OF FIGURES (Cont)

## LIST OF FIGURES (Cont)

CONFIDENTIAL

## CONFIGURATION – D181-960-009

6 Allison 550-B-1
Engines

1172 (97'-8")

407. (33'-11")

CONFIDENTIAL

973 (81'-1")

1/200 SCALE

Computer and Cockpit Set-Up

ABSTRACT

A brief preliminary analysis is presented in this report of the hovering and transition stability, and an insight to the reaction control picture associated with one of the more promising design configurations of a ducted fan vertical take-off and landing assault transport airplane. These analyses are introductory in nature and tend to define feasibility and areas for further study.

Concentration of effort has been placed primarily on hovering flight where the aerodynamic forces are assumed negligible and only engine gyroscopic, duct fan characteristics, mass and inertia terms are important. The hovering condition was investigated with various control levels for control stabilizing the airplane while individual gusts as high as 50 feet per second were applied in roll, pitch and yaw. A "pilot acceptable" gradient was determined after many hours of simulated flight time on the Reeves Electronic Analogue Computer. REAC traces are shown of pilot input and resulting airplane output displacements as a function of time for the various conditions studied.

Transition phase where the aerodynamic forces tend to build up with increasing velocity proves to be of less importance in comparison to hovering. Here conventional aerodynamic control surfaces tend to become effective with increasing velocity and tend to augment the reaction controls at the low flight speeds.

Power off static longitudinal, lateral and directional stability has been investigated and horizontal and vertical tail sizes designed to give a desirable stability in pitch, roll and yaw.

## SUMMARY AND CONCLUSIONS

A preliminary analysis of the dynamics of hovering and transition flight has been investigated for a ducted fan configuration of a VTOL Assault Transport Aircraft. Emphasis is placed on the control hovering studies since these investigations represent the reaction control design criteria. Associated stability and control studies were also investigated for the transition phase of service flight. Analogue simulation of the aircraft dynamics along with a technique incorporating conventional airplane controls enabled Bell Aircraft Corporation test pilots to give "pilot opinion" concerning satisfactory and unsatisfactory flying characteristics of various reaction control input levels. Records and traces of pilot and aircraft response are presented and briefly analyzed for purposes of feasibility and control design requirements.

From the hovering studies it was learned that the pilot was able to control stabilize the airplane under still air and severe gust conditions up to 50 feet per second in roll, pitch and yaw. The following control requirements were established:

(1) Roll reaction control 7.5 degrees/sec$^2$

(2) Pitch reaction control 10 degrees/sec$^2$

(3) Yaw reaction control 5 degrees/sec$^2$

Plots of the equivalent forces and moments required for these gradients are shown in the figures of this report. Inclusion of power on duct aerodynamic terms in the hovering dynamics indicated reduced airplane ground drift tendencies.

Preliminary analyses of duct exit flap controls have been examined for roll and yaw control with flap chords of one to three feet

in length. For pitch control the downward force exerted by a J-85 engine located at the vicinity of the vertical-horizontal tail junction gives sufficient control for pitch attitude. The J-85 reaction engine is capable of producing 2400 pounds of force for pitch control.

Transition cases were examined for representative speeds on take-off and landing. Aerodynamic control became more apparent to the pilot with the higher forward velocities. Traces are presented showing the pilots ability to avoid divergent motion for the various conditions investigated.

The horizontal and vertical tails were respectively designed to give an average static margin of 12% and a yaw stability level of approximately .0015/degree. The wing geometric dihedral is zero, with positive roll stability exhibited throughout.

The following conclusions may be drawn from these studies:

1. Acceptable control gradients can be designed for the AT Airplane.

2. Bell Aircraft Corporation pilots can control the airplane manually in hovering flight with the acceptable control gradients established.

3. Pitch reaction control can be obtained from a J-85 engine situated at the tail end of the fuselage.

4. A split flap type control arrangement at the duct exit is satisfactory for roll control.

5. Yaw controls for hovering flight can be designed as a ducted flap arrangement or a reaction engine at the tail.

6. Static longitudinal stability is ample and of proper order for service level-flight conditions.

7. Lateral – directional stability is ample throughout the level flight regime.

8. Inherent engine gyroscopic moments tending to couple the pitch and roll planes of the airplane prove to be of little consequence to the pilot for the hovering and transition cases studied.

9. Fan slipstream effects on the horizontal tail are negligible.

10. Large moments of inertia of the AT Airplane result in a relatively easily control stabilized airplane.

The following recommendations are suggested for future stability and control studies:

1. Detailed studies along with a wind tunnel program of the duct – exit flap controls should be made for proper design refinement.

2. Control lag studies should be made for the dynamic hovering and transition studies on the REAC.

3. Level flight dynamic stability should be investigated throughout the conventional flight regime.

4. A flight simulator program should be initiated to include a complete flight from hovering to transition with a pilot flying a given flight path.

5. A complete wind tunnel program should be initiated to cover power on and power off aerodynamic characteristics of the airplane.

─── **B E L L** *Aircraft* CORPORATION ───

6.  A detailed investigation of maneuverability of the VTOL AT
    Airplane should be conducted.

7.  A comprehensive study of power on and power off duct aero-
    dynamics should be made with wind tunnel substantiation.

8.  Feasibility study of controlling duct aerodynamics by inlet
    boundary layer control and possible resulting applications
    to aircraft control.

## PART I

### INTRODUCTION

For the past five years Bell Aircraft Corporation has been studying the feasibility of horizontal attitude - vertical take-off and landing airplane configurations. A test vehicle has been built and flown successfully utilizing rotation of jet engines for hovering and transition. Another test vehicle is now being built incorporating jet tail exit rotation. This report presents preliminary paper studies on a ducted fan vertical take-off assault transport airplane again with the initial take-off in the horizontal attitude. Studies covering the more pertinent stability and reaction control problems associated with ducted fan VTOL aircraft are considered for the most promising AT design studies to date.

The results presented herein are felt to be indicative of the airplane, although better quantitative data should be obtained from wind tunnel and/or flight testing. Since under the contract a brief study was desired, detailed comprehensive studies and analyses are not presented, but rather the associated problem of feasibility.

This airplane has a gross weight of 67,660 pounds and an empty weight of 42,390 pounds. The ducted propellers, powered by Allison engines, are situated at the extreme wing tips with the smaller diameter ducts situated slightly inboard. The ducts are located so that the horizontal tail is unaffected by the slipstream of the ducted propellers.

The wing incorporates zero sweep of the quarter chord with an effective aspect ratio of 5.8 and a taper ratio of three quarters. The horizontal and vertical tail are respectively 310 and 232 square feet with

aspect ratios of 4.35 and 1.82. Both surfaces have 65A – 008 airfoil sections with leading edge sweep of the vertical tail equal to 25 degrees and four degrees for the horizontal tail.

Jet reaction control has been considered for pitch (also yaw) from a J-85 engine located at the tail end of the fuselage and flap control situated at the duct exit for roll and yaw control during hovering. Other types of roll and pitch control have been considered but not developed due to the dearth of ducted fan aerodynamics. For example it is possible that the duct forces and moments might be developed at will by injecting compressed air at the duct inlets giving a primary or supplementary method of control. A thorough wind tunnel program is necessary to give the designer an understanding of the potentials of ducted fan propulsion.

## PART II

### HOVERING AND TRANSITION STABILITY AND CONTROL

In 1952 the Bell Aircraft Corporation instituted a general program devoted to VTOL stability and control problems. Generalized stability equations were developed to describe an aircraft in hovering and transition flight. The development of the equations of motion are given in these works (References 4, 5 and 6) and are not presented herein.

Analytical Treatment:

In utilizing the basic equations of motion for the dynamics in hovering flight the following assumptions were made:

    a. The aircraft was assumed rigid

    b. Aerodynamic forces and moments were of negligible magnitudes

    c. Only small angles existed in roll, yaw and pitch

    d. Initially the aircraft velocities and displacements are zero

    e. Reaction control produced pure couples

    f. Thrust level of ducts remained constant

In considering that the thrust level remained constant, it was assumed that pitch and roll controls did not effect the overall thrust. Brief studies were conducted to determine the effect of this assumption on the present system and it was found that the thrust to weight ratio would have to be maneuvered between approximately 1 and 1.025 to maintain a pre-determined altitude. In the time available it was not possible to incorporate pilot control studies of thrust on the analogue simulator.

Two axes systems were used for the equations. Moment equations utilized body axes with origin at the center of gravity, the X axis parallel to the fuselage center line, and the Y axis parallel to the wings. The force equation coordinate system also had its origin at the center of gravity but the XY plane remained parallel to the ground plane while the X axis was oriented to the azimuth heading of the aircraft. This gave the advantage of having forward and lateral velocities parallel to the ground plane.

The resulting equations for hovering are:

Forces:

$$\overset{o}{u} = \frac{T}{m} \theta$$

$$\overset{o}{v} = \frac{T}{m} \phi$$

$$\overset{o}{w} = \frac{T}{m} - \frac{T}{m} \cos \theta \sin \phi$$

Moments:

$$\frac{L_{(t)}}{I_x} = \ddot{\phi} + \frac{j_3}{I_x} \dot{\theta} - \frac{I_{xz}}{I_x} \ddot{\psi}$$

$$\frac{M_{(t)}}{I_y} = - \frac{j_3}{I_y} \dot{\phi} + \ddot{\theta} + \frac{j_1}{I_y} \dot{\psi}$$

$$\frac{N_{(t)}}{I_z} = - \frac{I_{xz}}{I_z} \ddot{\theta} - \frac{j_1}{I_z} \dot{\theta} + \ddot{\psi}$$

where:

      a.  All angles are in radian

      b.  $I_x$, $I_y$, $I_z$ and $I_{xz}$ represent the moments of inertia and product of inertia respectively.

      c.  $j_1$, $j_2$, $j_3$ represent the components of the total angular momentum vector along the X, Y and Z axes.

      d.  T is the thrust in pounds

      e.  $L(t)$, $M(t)$, and $N(t)$ represent the reaction control moments pound feet.

## Gyroscopic Effects:

In previous low density configuration studies of airplane hovering and transition, engine gyroscopic effects have been considered of first order importance. For the -007 and -009 assault transport designs the large airplane moments of inertia decreased the importance of the engine effects. In the computer hovering studies the pilot was almost unaware that gyroscopic coupling existed in pitch and roll. Figure 1 is included to indicate the gyroscopic angular accelerations developed in roll and pitch due to $\dot{\theta}$ and $\dot{\phi}$, with engines developing maximum power and duct rotation equal to 90 degrees.

## REAC Studies:

The "hovering flight" conditions have been investigated for the D-181 designs 007, 009 and also a 009 modified design (which is that as shown in the three view drawing). The assault transport VTOL ducted fan designs were investigated for landing and take-off service conditions. The primary purpose of this preliminary design study was to establish control

force gradients required for the reaction control system in roll, pitch and yaw and thus determine the reaction control design feasibility for satisfactory hovering and transition flight.

Evaluation of the hovering stability characteristics and control requirements were carried out principally by analogue simulation. The computer set up was made on the basis of linear and angular inertial equations including the gyroscopic effects of the engine. Provisions were made to introduce simulated reaction control quantities from a stick-pedal arrangement into these equations. Similarly the output of the computer was presented to the pilot, on two oscilloscopes, thereby giving him aircraft attitude and velocity information. During the tests random gusts were interjected by the computer operator and the resultant pilot and airframe response recorded.

The stick-pedal mockup provided with three potentiometers to measure electrically the angular displacements of the controls. Since the reaction controls were assumed to vary linearly with control displacement the electrical angular displacement signals were merely amplified to the desired level and fed into the computer problem as angular acceleration, i.e., $\frac{L(t)}{I_x}$ , etc.

In testing the system the computer was first calibrated for a given weight and control level. The pilot would then "hover", first with no gusts, followed by simulated flights corresponding to variant gust conditions. Since the gusts were considered to give pure couples the only disturbance indication available to the pilot was a change and rate of change of attitude. This partially accounts for the pilot's use of the

"attitude" oscilloscope as a primary information source. Several control levels were used with each of two test weights.

During the tests the airframe was disturbed by random pulse shaped gusts of one second time duration. It is felt that pulse shaped gusts are representative of the most drastic type that could be encountered. The resulting variation of $u$, $v$, $\phi$, $\theta$, $\psi$, $\ddot{\theta}$ and $\ddot{\phi}$ as well as pilot response and gust conditions were continuously recorded during each run. After each gust the pilot corrected his attitude and then zeroed his velocity.

The computer program was set up such that aircraft weight, control level, and gust magnitudes were varied. Upon completion of this program (see Table of Computer Studies) a satisfactory "pilot acceptable" reaction control level was arrived at from which the necessary forces and moments were determined.

In both weight tests the gyroscopic coupling that existed between roll and pitch was small and therefore only barely noticeable to the pilot. As a consequence the large moments of inertia result in a relatively easy "control stabilized" aircraft.

Rolling and pitching motions were periodic and had a common period of 114 seconds for the maximum weight condition and 113 seconds for the light weight condition.

Figures 2 and 3 show the effect of control gradients on the hovering lateral and longitudinal dynamics with a roll gust of 50 ft/sec and control gradients numbered 1, 2 and 3. (See Table II-1). The gross weight condition of 67,660 pounds is shown in Figure 2; $\ddot{\psi}$, $\ddot{\phi}$, and $\ddot{\theta}$ are the pilot control inputs utilized for correcting the gust disturbance. The

"pilot acceptable" gradient is that indicated as No. 2. Although gradient
No. 1 indicates better control stability the Bell Aircraft Corporation
test pilots indicated that gradient No. 2 was acceptable, thus lowering
the control requirements. Figure 3 shows the effect of the lighter air-
plane weight of 42,390 pounds. Figure 4 gives an indication of weight or
inertia effects on the airplane. Figure 5 indicates the severity of the
different gusts in pitch, yaw and roll on the lateral and longitudinal
dynamics. The traces indicate that the roll gust seems to be the more
difficult to control for the pilot than the yaw gust as shown in the lateral
dynamics. Figure 6 shows the same traces for the lighter weight condition.
Figures 7 (a) and (b) show the dynamics respectively for the heavy and
light weights with the pilot acceptable gradients controlling airplane at-
titude with gust magnitudes of 30 feet per second in roll pitch and yaw.

Hovering Stability with Power On Duct Aerodynamics:

During the latter part of the studies the aerodynamic effects of
the ducts, inboard and outboard with full power on (see Figure 8) were inclu-
ded in some of the hovering dynamic studies. It was found that, although
the "fixed stick" characteristics went from a neutrally stable category to
an unstable category, the aircraft appeared more easily controlled by the
pilot. Drift velocities over the "ground" were reduced. This increase in
"control stability" is of course accompanied by greater pitch control re-
quirement for maneuvering. For these tests ten degrees per second squared
was used for pitch control representing approximately two thirds of the
total angular acceleration available using the J-85 engine at the tail.

D-181-960-009

## REAC "HOVERING" COMPUTER STUDIES

| Condition | Grad.# | Reaction Control | Gust Magnitudes |
|---|---|---|---|
| Take-Off - Wt. = 67,660# | 1 | Roll; 10° per second sq.<br>Pitch; 15° per second sq.<br>Yaw; 7.5° per second sq. | Zero to 50 ft. per second in roll, pitch, and yaw |
| Do | *2 | Roll; 7.5° per second sq.<br>Pitch; 10.0° per second sq.<br>Yaw; 5.0° per second sq. | Do |
| Do | 3 | Roll; 5° per second sq.<br>Pitch; 10° per second sq.<br>Yaw; 5° per second sq. | Do |
| Do | 4 | Roll; 6.5° per second sq.<br>Pitch; 10.0° per second sq.<br>Yaw; 5.0° per second sq. | 50 ft/sec roll gust |
| Do | 5 | Roll; 8.5° per second sq.<br>Pitch; 10.0° per second sq.<br>Yaw; 5.0° per second sq. | Do |
| Landing - Wt. = 42,390# | 1 | See corresponding reaction controls | Zero to 50 ft. per second in roll, pitch, and yaw |
| Do | *2 | | Do |
| Do | 3 | | Do |

* Pilot Acceptable Gradient

In computing the duct moments and normal forces, a dimensional analysis was made to determine possible empirical expressions for these quantities. Upon determining those expressions that most closely fit the data of Reference 24, the approximations of the moments and normal forces were made. Specifically those moments and forces corresponding to angles of attack of 80, 85 and 90 degrees with a free stream velocity of 0 to 30 feet were calculated. Wind tunnel tests are presently being conducted at the University of Wichita which should result in better approximations of these quantities.

Reaction Control:

From the foregoing tests (with and without duct aerodynamics) it appeared that a control level of 7.5 $deg/sec^2$ in roll, 10 $deg/sec^2$ in pitch and 5 $deg/sec^2$ in yaw was sufficient for control. In order to provide these control gradients it would be necessary to provide maximum forces of 3650 pounds at the center line of one outboard duct for roll, 1540 pounds at the J85 tail exhaust for pitch, and 2250 pounds at the center line of one outboard duct for yaw. To attain these forces a system of split flaps and plain flaps at the exit of the outboard ducts for roll and yaw, respectively was examined. The split flaps used for roll and the plain flap for yaw control.

The design incorporates a J-85 engine for pitch reaction control which is capable of producing a force of approximately 2450 pounds. Figure 10 presents design reaction control moments required for various control gradients. Figure 11 shows the forces required for pitch control with the various gradients. Estimates of the yaw and roll flap reaction controls
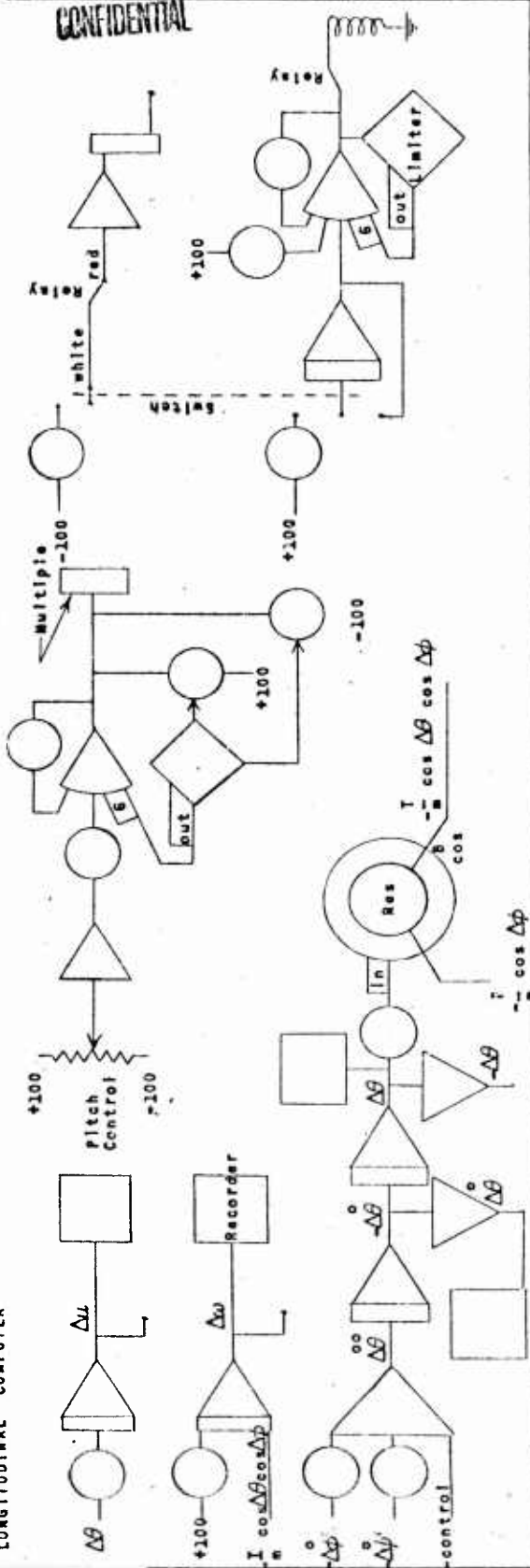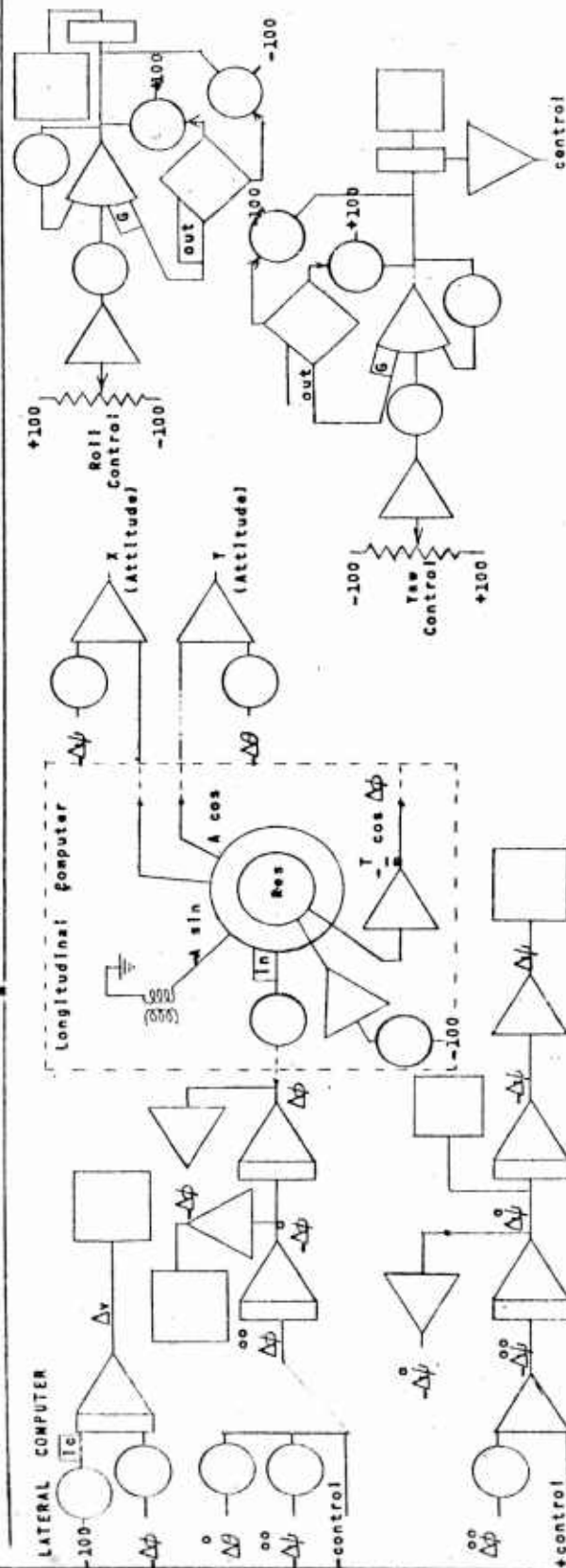
CONFIDENTIAL

D181-960-009   HOVERING SCHEMATIC

Form E4-1 Rev. 353

required for various input gradients are shown respectively in Figures 12 and 13. Assuming yaw control at the tail, Figure 12 (b) shows the amount of force required for acceptable control. The moment arm is the distance from the cg to the force action point. Figure 14 shows the yaw control forces and moments developed by outboard duct exit flaps of 1, 2, and 3 foot chords. Engine power is maximum and corresponding duct exit velocity equal to 390 ft/sec. The forces and moments are calculated for control deflections up to 25 degrees. Figure 15 indicates the roll reaction control forces developed by split flaps situated at the duct exit for duct exit velocities of 305 and 390 feet per second and control flap chords of 1 - 3 feet with split flap deflection angles up to 40 degrees.

Transition:

The need for a transition stability and control analysis, although not as critical as a dynamic analysis for hovering, is necessary for developing the aircraft pilot response at low speeds to gust conditions. During a typical transition, aerodynamic moments and forces rapidly come into play representing a period during which engine gyroscopic moments become comparatively insignificant to those of an aerodynamic nature. Hence, although damping and pilot control is continually improving, the oscillatory modes must be checked.

In studying transition, four transition cases were investigated and the pilot's ability to fly these service conditions were checked by the classical perturbation technique. Before putting these problems on a computer for analogue simulation it was necessary first to make certain simplifying assumptions dictated to a great extent by time availability. With the exception of excluding duct power moments none of these simplifications

seem critical when considering the overall objectives. Sufficient data was not available at the time to determine power on ducted fan effects.

Analogue simulation of the equations of motion was set up on a Reeves Computer and pilot control introduced therein. As in hovering the pilot was given attitude information on the oscilloscopes with a conventional stick and pedal arrangement for corrective measures. Aircraft motion variables as well as pilot control response was recorded for various gust conditions.

Following is a list of the simplifying assumptions made:

1. The aircraft is a completely rigid structure.

2. The reaction control axes coincided with the aerodynamic control axis. Since the angles of attack encountered were small, this was considered satisfactory.

3. The initial values of the basic variables $\theta$, $\alpha$, $\Delta\alpha$, $\beta$, $\phi$, $\psi$ and their derivatives are zero.

4. The small angle assumption was made for $\phi$, $\theta$, $\psi$ and $\alpha$.

5. The aircraft was symmetrical to the XZ plane both from a weight and aerodynamic standpoint.

6. The X moment axis initially coincide with the X force axis.

7. V is small compared with $V_o$.

8. No duct rotation with respect to the airframe takes place during the problem.

9. The aircraft is initially trimmed.

10. Duct power moments and normal forces were neglected.

Equations of Motion:

Following are the basic equations used for this analysis. Develop-
ment of these equations can be found in Bell Aircraft Corporation Report No.
65-978-002.

$$
\begin{bmatrix}
D+K_1 & K_2 & K_3 & 0 & 0 & 0 \\
K_4 & D+K_5 & -D+K_7 & 0 & 0 & 0 \\
K_8 & K_9 & D^2+K_{10}D & 0 & K_{22}D & K_{21} \\
0 & 0 & 0 & D+K_1' & K_0'D-K_2' & 1 \\
0 & 0 & K_{23}D & K_3' & D^2+K_4'D & -K_5'D-K_6' \\
0 & 0 & K_{24}D & -K_7' & -K_8'D^2-K_9'D & D+K_{10}'
\end{bmatrix}
\begin{bmatrix}
\dfrac{\Delta U}{U_o} \\[2mm]
\Delta \alpha \\[2mm]
\Delta \theta \\[2mm]
\Delta \beta \\[2mm]
\Delta \phi \\[2mm]
\Delta \dot{\psi}
\end{bmatrix}
=
\begin{bmatrix}
0 \\
0 \\
G_3(t) \\
F_1(t) \\
F_2(t) \\
F_3(t)
\end{bmatrix}
$$

Where

$$K_1 = \frac{2}{\tau} C_{D_0}$$

$$K_2 = -\frac{g}{U_o} + \frac{C_{D_\alpha}}{\tau} + \frac{T}{mU_o} \sin(\lambda + \alpha)$$

$$K_3 = \frac{g}{U_o}$$

$$K_4 = \frac{2C_{Lo}}{\tau}$$

$$K_5 = \frac{T}{mU_o} \cos(\lambda + \alpha_o) + \frac{C_{L_\alpha}}{\tau}$$

$$K_7 = 0$$

$$K_8 = 0$$

$$K_9 = -\frac{C_{m_\alpha}}{I_Y} qSc$$

$$K_{10} = -\frac{1}{\tau} \frac{C_{m_q}}{I_Y} \left(\frac{qSc^2}{2U_o}\right)$$

$$K_1' = - \frac{C_{Y_\beta}}{\tau}$$

$$K_2' = \frac{g}{U_o}$$

$$K_3' = - \frac{C_{l_\beta}}{I_X} \ (qSb)$$

$$K_4' = - \frac{C_{l_P}}{I_X} \ (\frac{qSb^2}{2U_o})$$

$$K_5' = \frac{I_{XZ}}{I_X}$$

$$K_6' = \frac{C_{l_r}}{I_X} \ (\frac{qSb^2}{2U_o})$$

$$K_7' = \frac{C_{n_\beta}}{I_Z} \ (qSb)$$

$$K_8' = \frac{I_{XZ}}{I_Z}$$

$$K_9' = \frac{C_{n_p}}{I_Z} \ (\frac{qSb^2}{2U_o})$$

$$K_{10}' = \frac{C_{n_r}}{I_Z} \ (\frac{qSb^2}{2U_o})$$

$$K_O' = \frac{C_{Y_p}}{2\mu'}$$

$$K_{21} = \frac{J \cos (\alpha + \bar{\lambda})}{I_Y}$$

$$K_{22} = \frac{J \sin (\alpha + \bar{\lambda})}{I_Y}$$

$$K_{23} = \frac{J \sin (\alpha + \bar{\lambda})}{I_X}$$

$$K_{24} = \frac{J \cos (\alpha + \bar{\lambda})}{I_X}$$

$\overline{\lambda}$ = angle measured from wing root chord to engine angular momentum vector

$\lambda$ = angle measured from wing root chord to thrust line

$$\tau = \frac{m}{\frac{1}{2}\rho U_o S}$$

$C_{L_O}$, $C_{D_O}$ = initial value of $C_L$ and $C_D$

$$G_3(t) = \left\{\frac{mU_o c}{I_Y \tau} C_{m_{\delta_e}}\right\} \delta_e + \frac{\text{Pitch Reaction Control Moment}}{I_Y}$$

$$F_1(t) = \left(\frac{1}{\tau} C_{Y_\delta}\right) \delta_r$$

$$F_2(t) = \left\{\frac{mU_o b}{I_X \tau} C_{l_\delta}\right\} \delta_a + \frac{\text{Roll Reaction Control Moment}}{I_X}$$

$$F_3(t) = \left\{\frac{mU_o b}{I_Z \tau} C_{n_{\delta_r}}\right\} \delta_r + \left\{\frac{mU_o b}{I_Z \tau} C_{n_{\delta_a}}\right\} \delta_a + \frac{\text{Yaw Reaction Control Moment}}{I_Z}$$

The above equations were simulated on an analogue computer (see computer transition schematic) with the control parameters being generated by the pilot using a control system mockup. The pilot's primary presentation consisted of a bar on an oscilloscope that moved up and down for pitch, left and right for sideslip and tilted for roll. A secondary presentation gave the pilot yaw information. One second gusts corresponding to 50 feet per second air velocity were introduced by giving suitable angular accelerations in yaw, pitch or roll.

The following points of possible transition were taken as test points:

| Case | $U_o \frac{ft}{sec}$ | $a$, deg | $\lambda$, deg | T, lbs | Weight, lbs |
|------|------|------|------|------|------|
| I | 118.7 | 8 | 80 | 51,413 | 67,660 |
| II | 22.93 | 4 | 80 | 67,660 | 67,660 |
| III | 122.9 | 8 | 40 | 67,660 | 67,660 |
| IV | 170.8 | 4 | 40 | 67,660 | 67,660 |

In making the above analysis the reaction control level was taken as; 10 degrees per second$^2$ in pitch, 7.5 degrees per second$^2$ in roll and 5 degrees per second squared in yaw. To these reaction control angular accelerations was added the aerodynamic control angular accelerations corresponding to the initial $U_o$ involved. Since $\frac{\Delta U}{U_o}$ remained small, this was quite accurate. In all cases the stability was improved over that in hovering, and with the exception of Case II, the control improvement was readily recognized by the pilot. As in hovering the gyroscopic effects could hardly be noted. The results of three runs of Case IV are shown in Figures 16 to 21 inclusive illustrating the ease of control stabilizing at this speed.

BELL *Aircraft* CORPORATION

Aerodynamic Control Derivatives Used on REAC Transition Studies

Rudder:

$$C_{Y_{\delta_r}} = .00378/\text{deg} \qquad (\alpha = 4 \ \& \ 8°)$$

$$C_{n_{\delta_r}} = -.00155/\text{deg} \qquad (\alpha = 4 \ \& \ 8°)$$

Elevator:

$$(C_{m_{\delta_e}}) = .00695/\text{deg} \qquad (\alpha = 4.0)$$

$$(C_{m_{\delta_e}}) = .00576/\text{deg} \qquad (\alpha = 8.0)$$

$$(C_{L_{\delta_e}}) = -.00268/\text{deg} \qquad (\alpha = 4.0)$$

$$(C_{L_{\delta_e}}) = -.00218/\text{deg} \qquad (\alpha = 8.0)$$

Aileron:

$$(C_{l_{\delta_a}}) = .00129/\text{deg} \qquad (\text{one aileron} - \alpha = 4 \ \& \ 8°)$$

Adverse Yaw Due to Aileron:

$$C_{n_{\delta_a}} = .0043/\text{deg} \qquad (\alpha = 4)$$

$$C_{n_{\delta_a}} = .007/\text{deg} \qquad (\alpha = 8.0)$$

**CONFIDENTIAL**

**CONFIDENTIAL**

D181-960-009
TRANSITION SCHEMATIC

R: Resolver

▢: Multiple

◻: Recorder channel

◇: Limiter

## PART III

### STATIC LONGITUDINAL STABILITY

A brief study of the longitudinal stability of the ducted fan assault transport has been made to determine the horizontal tail size required for an adequate airplane static margin. The horizontal tail was designed for an approximate static margin of -.12 for the low speed and lift coefficient range. The aerodynamic data necessary for the computations of the pitching moments are presented within the body of this report – such as the wing and horizontal tail lift curve slopes, downwash, and the destabilizing effect of the fuselage and ducts. The most aft cg has been used throughout for the computations. This cg corresponds to 17.6% of the wing mean aerodynamic chord and represents the fully loaded weight condition. The deviation in cg position between the heavy and light weights is exactly 1.0 inch. The assumption has also been made that the center of pressure of all surfaces is at the quarter chord of the mac.

### Horizontal Tail Geometry Characteristics:

The horizontal tail geometric characteristics are shown in Figure 22. Horizontal tail area is 310 square feet and is 25% of the reference wing area. The leading edge sweep is 13.75 degrees and the taper ratio equal to .52. The aspect ratio of the horizontal tail based on the leading and trailing edges of the horizontal tail extended to the center line of the fuselage is 4.35. The lift curve slope of the horizontal tail is based on this aspect ratio, with reductions in lift curve slope due to cutouts and interference based on AAF TR 5167, from Reference 25. The lift curve slope for the horizontal tail is given in Figure 23 along with the wing and vertical tail lift curve slopes.

The fuselage and wing characteristics can be seen from the three-view drawing.

The static longitudinal stability was determined by summing up the various contributions of the airplane components. Perusal of the slip-stream effects due to the inboard ducts indicate a negligible/or beneficial effect for steady symmetric flight conditions. The following contributions to the longitudinal stability have been considered for the airplane:

$$(C_{m_\alpha})_A = (C_{m_\alpha})_F + (C_{m_\alpha})_{D_{in}} + (C_{m_\alpha})_{D_o} + (C_{m_\alpha})_{HT} + (C_{m_\alpha})_W$$

and the static margin is:

$$\frac{dC_m}{dC_L} = (C_{m_\alpha})_A \div (C_{L_\alpha})_A$$

Fuselage and Duct Contribution:

The fuselage, inboard and outboard ducts (see Figure 24) were the only destabilizing components and were estimated by an empirical expression given in Reference 22 as follows:

$$(C_{m_\alpha})_F = .01658 \ (K'') \ \left[\frac{S_T \ L_F}{(Sc)_{ref}}\right]\sqrt{\frac{h_1}{h_2}} \ \sqrt[3]{\frac{w_2}{w_1}}$$

$$(C_{m_\alpha})_D = .01658 \ (K''') \ \left[\frac{S_T \ L_F}{(Sc)_{ref}}\right]$$

<u>Wing Contribution:</u>

The wing contribution has been estimated by the following expression:

$$(C_{m_\alpha})_W = \frac{\overline{x}'}{c} (C_{L_\alpha})_W$$

Where:     $\overline{x}'$ = distance from cg to cp

c = wing mac

The contribution of wing, fuselage and ducts is shown in Figure 25.

<u>Horizontal Tail:</u>

The horizontal tail is computed by the following expression:

$$(C_{m_\alpha})_{HT} = (C_{L_\alpha})_{HT} \left(1 - \frac{d\epsilon}{d\alpha}\right) \left(\frac{q_H}{q_0}\right) \left(\frac{1_{HT}}{c}\right)$$

where the downwash has been estimated according to Reference 18. The variation of $\left(1 - \frac{d\epsilon}{d\alpha}\right)$ vs $(\alpha)$ is shown in Figure 26 for M = 0 and the horizontal tail contribution is shown in Figure 27. The variation of dynamic pressure at the horizontal tail has been taken as 0.9. Thrust moments have been neglected and been assumed to effect only a trim change on the airplane.

Figures 28 and 29 shows the stability respectively of the AT airplane in terms of $C_{m_\alpha}$ as a function of M and $C_L$ and static margin, $\frac{dC_m}{dC_L}$, as a function of M and $C_L$.

The reference aspect ratio for determining the lift curve slope of the wing has been taken from the center line of the airplane to the center line of the outboard duct which corresponds to a $(C_{L_\alpha})$ of equivalent aspect ratio of the exposed wing panels with body effects considered. The vertical tail has an effective aspect ratio greater than the geometric aspect ratio due to the low position of the horizontal tail and longitudinal location of the horizontal tail with respect to the vertical tail root chord. The vertical tail span is defined from the vertical tail tip to the horizontal tail plane. The horizontal tail lift curve slope was taken as shown in Reference 25, which indicates a reduction in lift curve slope due to the presence of tail cutouts, gaps, etc.

The Mach corrections were taken from the simple expression in Reference 26, and are functions of $\beta = \sqrt{1-M^2}$, $\Lambda$, and aspect ratio i.e.:

$$\frac{\left(C_{L_\alpha}\right)_M}{\left(C_{L_\alpha}\right)_{M=0}} = \frac{A + 2 \cos \Lambda}{AB + 2 \cos \Lambda} \quad (C_{L_\alpha})_{M=0}$$

## PART IV

### LATERAL DIRECTIONAL STABILITY

Directional Stability:

The static lateral directional stability characteristics of the VTOL ducted design were examined for the more pertinent Mach numbers and lift coefficients anticipated in conventional level flight. The following sections give a breakdown of the preliminary directional and lateral stability of the VTOL airplane. Throughout the service flight conditions positive stability is demonstrated throughout.

Vertical Tail Geometry:

The vertical tail has an aspect ratio of 1.82 where the span is defined as the distance from the tip extremity to the horizontal tail junction. Ratio of vertical tail area to wing reference area is 0.187, and sweep of the vertical tail leading edge is 25 degrees with a taper ratio of 0.297. Vertical tail airfoil section is a 65A series eight percent thick airfoil – identical to the horizontal tail. A sketch of the vertical tail geometry is shown in Figure 30. Figure IV-31 shows the lift curve slope of the vertical tail based on the wing reference area of 1240 square feet.

Fuselage Contribution:

Fuselage duct moments were estimated according to an empirical expression as given in Reference 22. The expression is identical to that used for the fuselage pitch instability, but different areas are used – i.e., the parameters are now in the yaw plane – the bodies still destabilizing. Calculations have been determined for $M = 0$, and it is assumed that the

Mach number has null effect. Due to the wings high position, the inter-
ference effect of the wing body combination contributes a stabilizing
effect and amounts to $C_{n_\beta}$ = .0002/deg.

Wing Contribution:

The wing contribution to $C_{n_\beta}$ of the airplane was estimated
according to References 9 and 26. The latter reference indicating the
effect of Mach number. It was found that the wing contribution was very
small for the low lift coefficients. The expression used is as follows:

$$(C_{n_\beta})_{M=0} = C_L^2 \left[ \left( \frac{C_{n_\beta}}{C_L^2} \right)_{\Lambda=0} - \frac{\tan \Lambda}{A(A+4\cos\Lambda)} \left( \cos\Lambda - \frac{A}{2} \quad \frac{A^2}{\beta \cos\Lambda} + 6\frac{\bar{x}}{\bar{c}}\sin\frac{\Lambda}{A} \right) \right]$$

the subsonic compressibility effects were estimated as shown below:

$$\left( \frac{C_{n_\beta}}{C_L^2} \right)_M = \left( \frac{A + 4\cos\Lambda}{AB + 4\cos\lambda} \right) \left( \frac{A^2 + 4AB\cos\Lambda - 8\cos^2\Lambda}{A^2 + 4A\cos^2\Lambda - 8\cos^2\Lambda} \right) \left( \frac{C_{n_\beta}}{C_L^2} \right)_{M=0}$$

Vertical Tail Contribution:

The positive contribution of the vertical tail to the directional
stability has been determined as follows:

$$(C_{n_\beta})_{VT} = (C_{L_\alpha})_{VT} \left( \frac{S_V}{S_{ref}} \right) (\eta_V) \left( \frac{l_V}{b_{ref}} \right)$$

The lift curve slope of the vertical tail was determined from Reference 9 and corrected for subsonic compressibility effects. The above reference also includes the end plate corrections due to the horizontal tail. The tail efficiency factor $\eta_V = \left(1 - \dfrac{d\sigma}{d\beta}\right)\left(\dfrac{q_V}{q_o}\right)$ is 0.9 throughout the analysis.

Airplane:

The total airplane stability is a summation of all the components and thus equal to:

$$(C_{n_\beta})_A = (C_{n_\beta})_F + (C_{n_\beta})_{D_o} + (C_{n_\beta})_{D_i} + (C_{n_\beta})_{VT} + (C_{n_\beta})_{int} + (C_{n_\beta})_W$$

The vertical tail has been designed to give a positive directional stability level of approximately $(C_{n_\beta})_A = .0015/\text{deg}$. In all cases the airplane shows positive directional stability. Figure 32 shows a plot of the contribution of the components, and Figure 33 the airplane directional stability.

Lateral Stability (Dihedral Effect):

The airplane exhibits small positive dihedral effect throughout the complete Mach number range. The wing incorporates approximately zero geometric dihedral angle. Wing contribution in itself exhibits small positive dihedral effect. The high wing location of the fuselage and the vertical tail contributes the largest positive stability effect.

Wing Position Effect:

Although the contribution of the fuselage alone to $C_{l_\beta}$ is usually negligible, the interference between the wing and fuselage can greatly alter the value of $C_{l_\beta}$. This interference is such that the high wing location gives more positive, $(-C_{l_\beta})$, effective dihedral. The expression for the wing position effect is

$$(C_{l_\beta})_{WP} = 1.2 \sqrt{A} \left(\frac{z}{b_{ref}}\right)\left( \right)$$

Wing Isolated Effect:

The simplified theory of Toll and Queijo (Reference 8) is used in obtaining the wing alone contribution to the rolling moment coefficient due to sideslip. The expression includes effects of sweep angle, aspect ratio, taper ratio, cg location and the additional increment of rolling moment due to sideslip which is proportional to the lift coefficient. The total deri-vative of the isolated wing with zero dihedral can be expressed as:

$$(C_{l_\beta})_{M=0} = \left[\left(\frac{C_{l_\beta}}{C_L}\right)_{M=0} - \frac{\bar{y}_{L_\beta}}{\left(\frac{b_W}{2}\right)} \left(\frac{A + 2\cos\Lambda}{A + 4\cos\Lambda}\right) \left(\frac{\tan\Lambda}{2}\right)\right]$$

Figure 34 shows this contribution as a function of Mach number. The sub-sonic compressibility effects were estimated from the following expression.

$$\left(\frac{C_{l_\beta}}{C_L}\right)_M = \left(\frac{A + 4\cos\Lambda}{AB + 4\cos\Lambda}\right) \left(\frac{AB + 2\cos\Lambda}{A + 2\cos\Lambda}\right) \left(\frac{C_{l_\beta}}{C_L}\right)_{M=0}$$

Vertical Tail Contribution:

Preliminary estimates of the vertical tail effective dihedral contribution were estimated according to the equation given below:

$$(C_{l_\beta})_{VT} = (C_{L_\alpha})_{VT} \left(\frac{S_{VT}}{S_{ref}}\right) \quad \left(1 - \frac{d\sigma}{d\beta}\right) \quad \left(\frac{q_V}{q_o}\right) \quad \left(\frac{z_V}{b_{ref}}\right)$$

Small negative values of $C_{l_\beta}$ are desired to improve the dutch roll damping characteristics whereas large negative values are desired for the spiral mode. Thus a compromise is required between static maneuvering lateral requirements of positive dihedral effect and the dynamic lateral requirements. Zero wing dihedral has been incorporated in the design to give a small positive dihedral effect. Figure 35 shows the variation of the airplane dihedral parameter with lift coefficient for $M = 0$ conditions.

Inboard Engine Out Trim Speed ($\phi = 0$):

Roll trim out speeds were calculated for one inboard engine out condition with wing trailing edge flap chord ratios of 25 and 50% and flap spans of 30 and 95% to give an indication of the type of aerodynamic aileron control that may be required. Figure 48 shows the roll trim out speeds for the aforementioned aileron span and chord configuration. Although the 50% aileron chord ratio is fictitious in the sense of practical design an insight as to what can be obtained is demonstrated. Reaction roll control moments are fixed for a $\ddot{\phi} = 7.5$ degrees/sec$^2$ (equivalent to $140 \times 10^3$ lb ft) with the wing trailing edge ailerons deflected $\pm20$ degrees.

PART V

DAMPING DERIVATIVES

Damping in Roll:

The damping in roll derivative $C_{l_p}$ is the change in rolling moment coefficient due to a change in rolling velocity. Large values of this parameter are desired for good dynamic stability. The wing gives the major contribution with the vertical and horizontal tail being of a second order nature – and these are generally unimportant unless these areas (and aspect ratios) run comparatively larger than conventional design dictates. The total damping in roll consisted solely of the wing contribution, with $C_L$ effects considered negligible. Damping in roll as a function of Mach number is shown in Figure 36 and estimated according to the following expression:

$$(C_{l_p})_{\substack{W \\ M=0}} = (C_{l_p})_{\Lambda=0} \left[ \frac{A + 4 \cos \Lambda}{(\frac{2\pi}{a_o}) A + 4 \cos \Lambda} \right]$$

where:

$$a_o = \text{section lift curve slope}$$

Corrected for compressibility effects:

$$(C_{l_p})_{\substack{W \\ M}} = \left[ \frac{A + 4 \cos \Lambda}{AB + 4 \cos \Lambda} \right]$$

where:

$$B = \sqrt{1 - M^2 \cos^2 \Lambda}$$

<u>Damping in Yaw:</u>

The damping in yaw, $C_{n_r}$, was estimated from the contribution of the wing plus vertical tail. The tail contribution is of the greater importance

$$\left(C_{n_r}\right)_A = \left(C_{n_r}\right)_{VT} + \left(C_{n_r}\right)_W$$

Figures 37, 38 and 39 give the contributions of respectively the vertical tail, wing and airplane.

<u>Damping in Pitch:</u>

The airplane damping in pitch parameter is composed of contributions from wing, tail, and fuselage. Since the wing and fuselage damping are small relative to the tail damping, conservatism results to assume the airplane damping in pitch is equal to the tail damping in pitch. Horizontal tail damping in pitch was calculated using the following expression:

$$\left(C_{m_q}\right)_{HT} \cong \left(C_{m_q}\right)_A = -2\left(C_{L_\alpha}\right)_{HT}\left(\frac{S_{HT}}{S_{ref}}\right)\left(\frac{l_t}{\bar{c}}\right)^2 57.3$$

Figures 41 through 44 show respectively the derivatives $C_{l_r}$, $C_{n_p}$, $C_{Y_p}$ and $C_{Y_r}$ required for the transition dynamic stability studies.

Estimates of the power off aerodynamic characteristics of the ducts are shown in Figures 45 through 47. These estimates are based primarily on the data from Reference 24.

## PART VI

### SYMBOLS

$C_{L_\alpha}$ ,     Lift curve slope

$C_{D_\alpha}$ ,     Drag curve slope

$C_{m_\alpha}$ ,     Pitch due to angle of attack

$C_{m_q}$,     Damping in pitch

$C_{Y_\beta}$ ,     Side force due to sideslip

$C_{Y_p}$,     Side force due to rolling angular velocity

$C_{Y_r}$,     Side force due to yawing angular velocity

$C_{n_\beta}$ ,     Yaw moment due to sideslip

$C_{n_p}$,     Yaw moment due to rolling angular velocity

$C_{n_r}$,     Yaw moment due to yawing angular velocity

$C_{l_\beta}$ ,     (Dihedral parameter) roll due to sideslip

$C_{l_p}$,     (Damping in roll), rolling moment due to rolling angular velocity

$C_{l_r}$,     Roll due to yawing angular velocity

$\ddot{\psi}$ ,     Yawing angular acceleration

$\ddot{\phi}$ ,     Rolling angular acceleration

$\ddot{\theta}$ ,     Pitching angular acceleration

$m$,     Mass $\dfrac{W}{g}$

$I_X$,     Roll moment of inertia

$I_y$,     Pitch moment of inertia

$I_z$,     Yaw moment of inertia

$I_{xz}$,     Product of inertia about x & z axis

$k_x$,     Roll radius of gyration

$k_y$,     Pitch radius of gyration

$k_z$, Yaw radius of gyration

$\tau$, $\dfrac{m}{\rho SU}$ , time conversion factor

$D$, $\dfrac{d}{d\tau} = \dfrac{d}{d\left(\frac{t}{\tau}\right)}$ , differential operator

$\mu$, $\dfrac{m}{1/2\,\rho\,Sb_W}$ , relative density factor

$u$, forward velocity ft/sec

$v$, sideslip velocity

$w$, vertical velocity

$\beta$, sideslip angle

$\theta$, pitch angle

$\phi$, roll angle

$\psi$, yaw angle

$\lambda$, angle from wing root chord to thrust line

$b$, wing span

$J$, angular momentum of engine

$T$, thrust

## PART VII

### REFERENCES AND BIBLIOGRAPHY

1.  Schetzer, J. D.: "Notes on Dynamics for Aerodynamicists". Douglas Aircraft Company, Inc. Report No. SM-14077, November 19, 1951

2.  Mitchell: "Dynamics of Aircraft Flight". Bell Aircraft Corporation Report No. 02-981-006, November 19, 1948

3.  BuAer Report DE-61-4: "Dynamics of the Airframe". Volume II, February 1952

4.  Roehrs, F.; Zabinsky, J. and O'Malley, J.: "A General Dynamic Stability and Control Analysis of Jet Powered VTOL Aircraft". Bell Aircraft Corporation Report No. 65-978-002 (Part I - AF-33(606-84)

5.  O'Malley, J.; Zabinsky, J. and Roehrs, F.: "Aerodynamics of the Bell VTOL Test Vehicle". Bell Aircraft Corporation No. 65-978-008, October 26, 1953

6.  Kane, J.; Vollo, S.; Roehrs, F. and Isom, J.: "Hovering and Transition Stability and Control". Bell Aircraft Corporation Report D-139-945-103, December 22, 1954

7.  Patterson, G. N.: "Ducted Fans, High Efficiency With Contra-Rotation". Report ACA - 10, October 1944

8.  Toll, T. A. and Queijo, M. J.: "Approximate Relations and Charts for Low Speed Stability Derivatives of Swept Wings". NACA TN 1501, May 1948

9.  Campbell, J. P. and McKinney, M. D.: "Summary of Methods for Calculating Dynamic Lateral Stability Response and for Estimating Lateral Stability Derivatives". NACA TN 2409

10. Pass, H. R.: "Analysis of W. T. Data on Directional Stability and Control". NACA TN 775, September 1940

11. Recant and Wallace: "Wind Tunnel Investigation of the Effect of Vertical Position of the Wing in the Side Flow in the Region of the Vertical Tail". NACA TN 804, April 1941

12. Thomson, F. L. and Gilruth, R. R.: "Notes on the Stalling of Vertical Tail Surfaces and on Fin Design". NACA TN 1940

13. Micheal, H. W.: "Investigation of Mutual Interference Effects of Several Vertical Tail Fuselage Configurations in Sideslip". NACA TN 3135, January 1954

14. Phillips, W. H.: "Appreciation and Prediction of Flying Qualities". NACA TR 927

15. Toll, T. A.: "Summary of Lateral Control Research". NACA TR 868, 1947

16. Sears, R. I.: "Wind Tunnel Data on the Aerodynamic Characteristics of Airplane Control Surface". NACA ACR 3L08 (L663), December 1943

17. Silverstein, A.; Katzoff, S.; and Bullivant, W. K.: "Downwash and Wake Behind Plain and Flapped Airfoils

18. Decker, J. L.: "Prediction of Downwash at Various Angles of Attack for Arbitrary Tail Locations". Preprint 615. Paper was presented at 24th Annual meeting of IAJ, January 23 - 26, 1956

19. Dods, J. B. and Tinling, B. E.: "Summary of Results of a Wind Tunnel Investigation of Nine Related Horizontal Tails". NACA TN 3497, July 1955

20. Neely, R. H. and Griner, R. F.: "Summary and Analysis of Horizontal Tail Contribution to Longitudinal Stability of Swept Wing Airplanes at Low Speeds"

21. Anderson, R. A.: "Determination of the Characteristics of Tapered Wings". NACA TR 527, 1936

22. Perkins and Hague: "Airplane Performance Stability and Control". John Wiley and Sons, 1949

23. Kucheman and Weber: "Aerodynamics of Propulsion". McGraw-Hill Book Co., 1953

24. Parlatt, L. P.: "Aerodynamic Characteristics of a Small Scale Shrouded Propeller at Angles of Attack From 0 - 90°". NACA TN 3547, November 1955

25. Perkins, C. D.: "Some Theoretical Developments in Airplane Static Longitudinal Stability and Control". AAF TR No. 5167, November 17, 1944

26. Fisher, L. R.: "Approximate Corrections for the Effects of Compressibility on the Subsonic Stability Derivatives of Swept Wings". NACA TN 1854, April 1949

GYROSCOPIC COUPLING EFFECTS OF ENGINES
IN HOVERING USING MAXIMUM POWER

D-181-960-009

Fig. No. I

EFFECT OF CONTROL GRADIENTS IN HOVERING
LATERAL DYNAMICS

D-181-960-009

D-181-945-005

WT. = 67,660 LBS

ROLL GUST = 50FT/SEC.

Fig.No.2(a)

CONFIDENTIAL

Control Gradients No. 1
Control Gradients No. 2
Control Gradients No. 3

CONFIDENTIAL

Page 41

EFFECT OF CONTROL GRADIENTS IN HOVERING
LONGITUDINAL DYNAMICS

D-181-960-009

D-181-945-005
Fig. No. 2(b)

WT. 67,660 LBS.

ROLL GUST — 50 FT./SEC.

CONFIDENTIAL

CONFIDENTIAL

Page 42

EFFECT OF CONTROL GRADIENTS IN HOVERING
LATERAL DYNAMICS

D-181-960-009

D-181-945-005
Fig. No. 3(a)

WT. = 42,390 LBS.

ROLL GUST = 50 FT./SEC.

CONFIDENTIAL

CONFIDENTIAL

D-181-960-009

EFFECT OF CONTROL GRADIENTS IN HOVERING
LONGITUDINAL DYNAMICS

WT. = 12,390 LBS.

ROLL GUST = 50 FT./SEC.

D-181-945-009
Fig. No. 5(b)

CONFIDENTIAL

Cont. Grad.
1
2
3
4

Gust

CONFIDENTIAL

Control

EFFECT OF LANDING AND TAKE-OFF WEIGHT IN HOVERING
LATERAL DYNAMICS

D-181-960-009

D-181-960-005
Fig. No. 4 (a)

Roll Gust = 40 Ft/Sec.

Pilot Acceptable Gradients

CONFIDENTIAL

42,390 Lb.
67,660 Lb.

CONFIDENTIAL
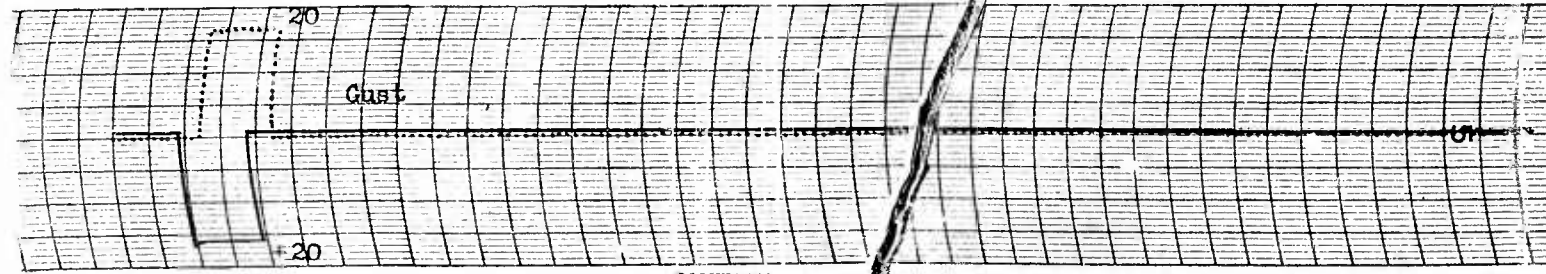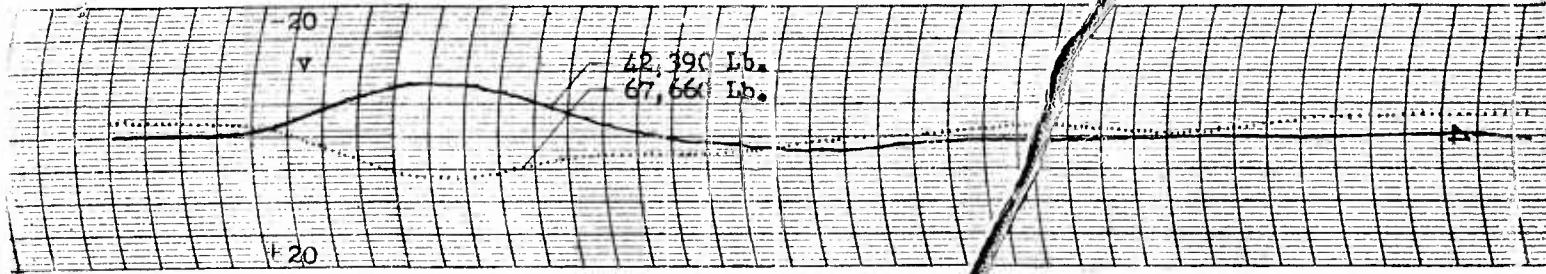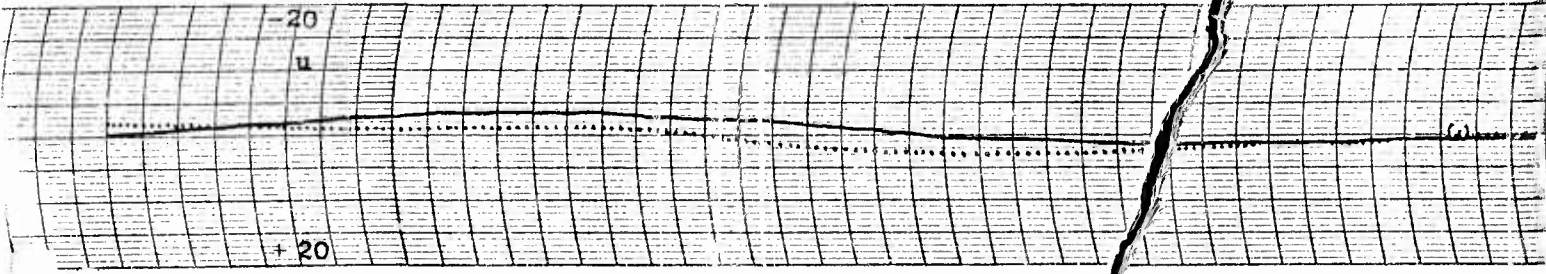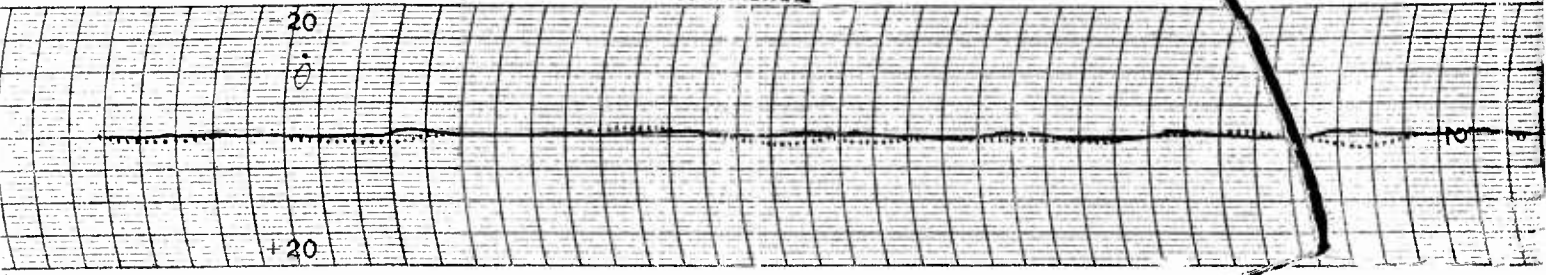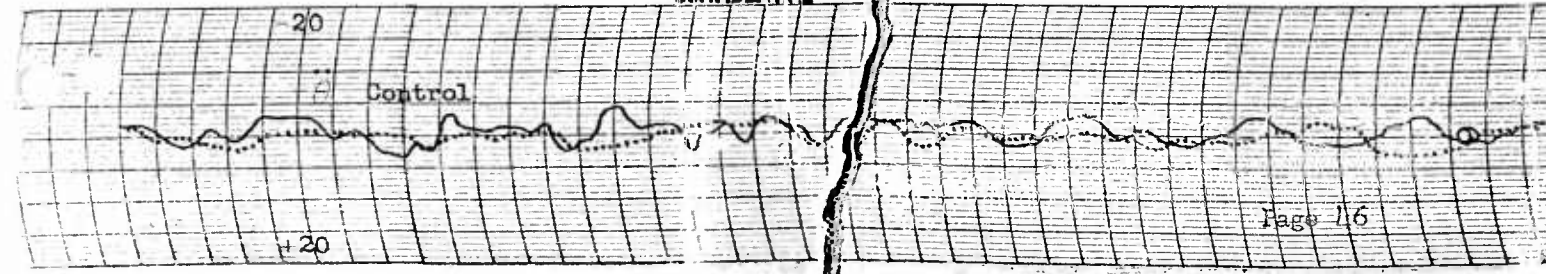
Page 45

EFFECT OF LANDING AND TAKE OFF WEIGHT IN HOVERING

LONGITUDINAL DYNAMICS

Roll Gust = 50 Ft/Sec.

Pilot Acceptable Gradients

−20
θ
+20

CONFIDENTIAL

−20
θ̇
+20

−20
u
+20

−20
v
+20

42,390 Lb.
67,660 Lb.

−20
Gust
+20

CONFIDENTIAL

−20
θ Control
+20

EFFECT OF ROLL, PITCH AND YAW GUSTS AT 50 FT./SEC. IN HOVERING
LATERAL DYNAMICS
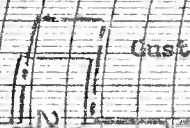
WT. = 67,660 LBS.

PILOT ACCEPTABLE
GRADIENT NO. 2

CONFIDENTIAL

CONFIDENTIAL

D-181-910-009

EFFECT OF ROLL, PITCH AND YAW GUSTS AT 50 FT/SEC. IN HOVERING

LONGITUDINAL DYNAMICS

WT. = 67,660 LBS.

D-181-915-005
Fig. No. 5(b)
PILOT ACCEPTABLE
GRADIENT NO. 2

$\theta$

$u$

$v$

Roll g
Yaw g
Pitch g

Gust

Control

Page 48

EFFECT OF ROLL, PITCH AND YAW GUSTS AT 50 FT./SEC. IN HOVERING

D-181-960-009

Fig. No. 6(a)

WT. = 42,390 LBS.

LATERAL DYNAMICS
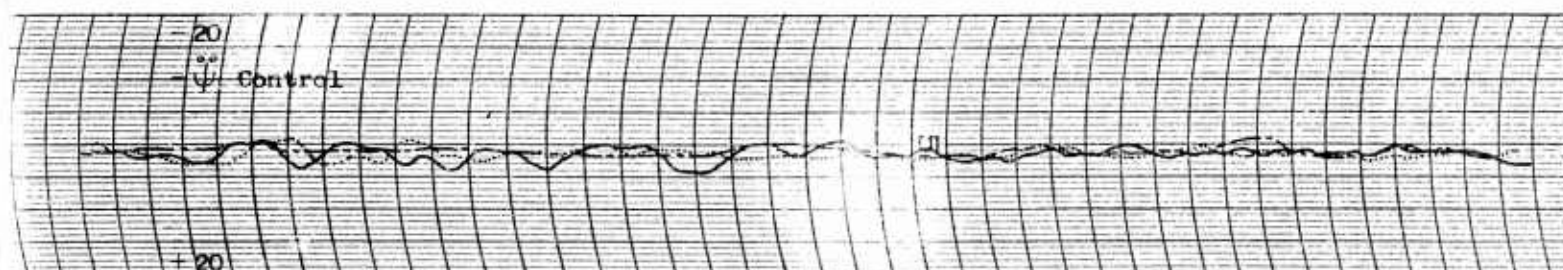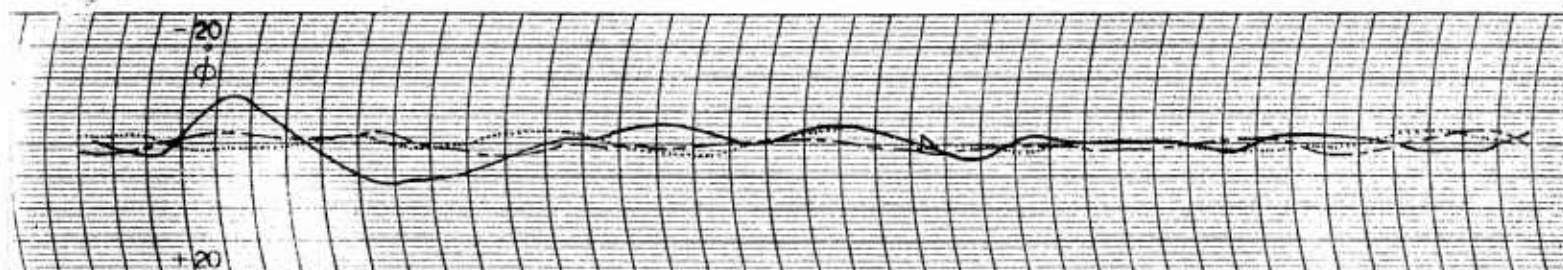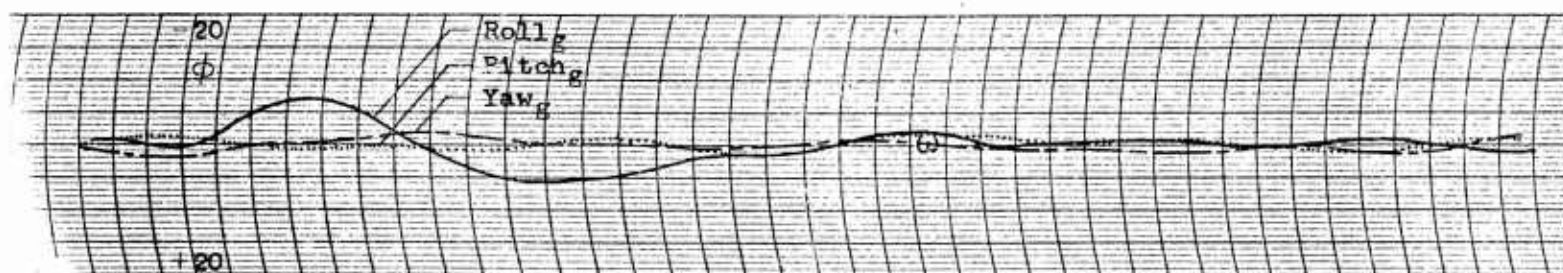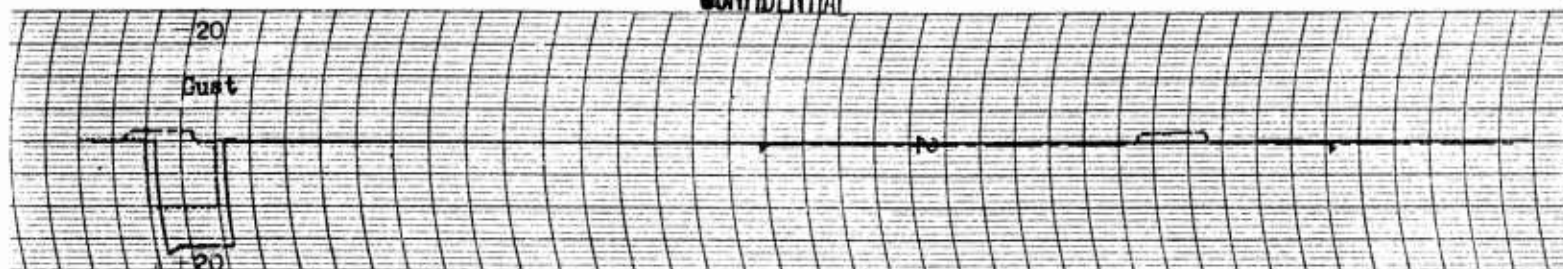
PILOT ACCEPTABLE
GRADIENT NO. 2

CONFIDENTIAL

CONFIDENTIAL

Page 49
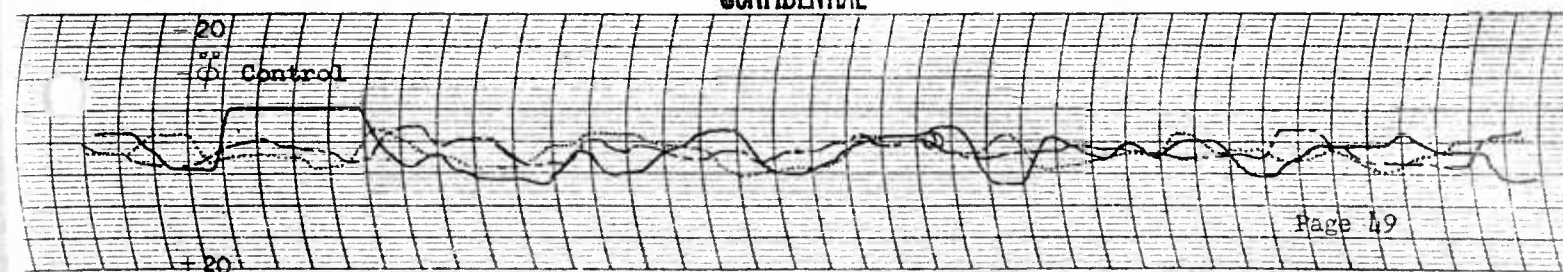
EFFECT OF ROLL, PITCH AND YAW GUSTS AT 50 FT/SEC. IN HOVERING
LONGITUDINAL DYNAMICS

D-181-960-009

D-181-945-009
Fig. No. 6(b)
PILOT ACCEPTABLE
GRADIENT NO. 2
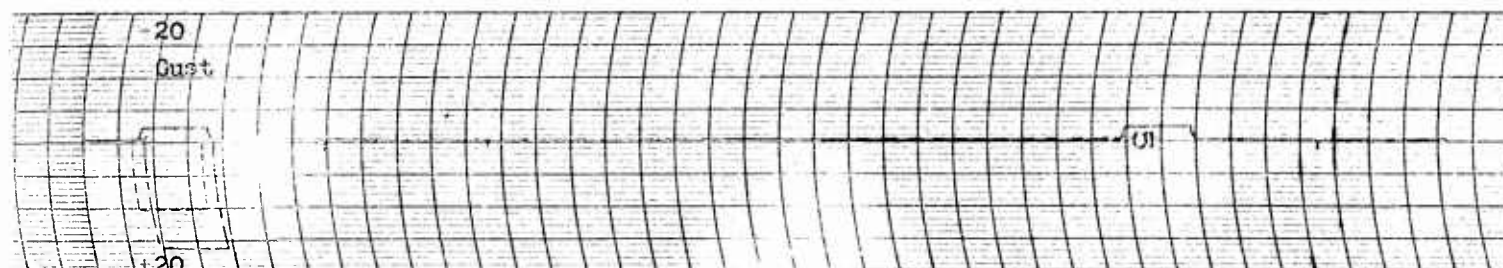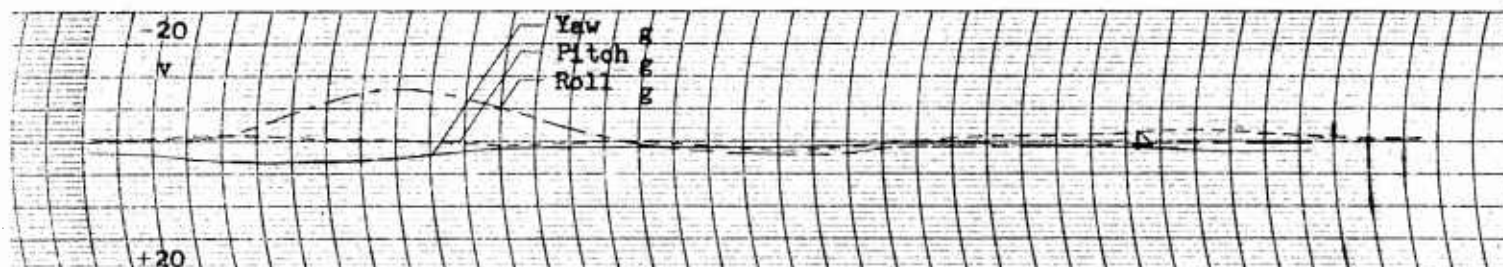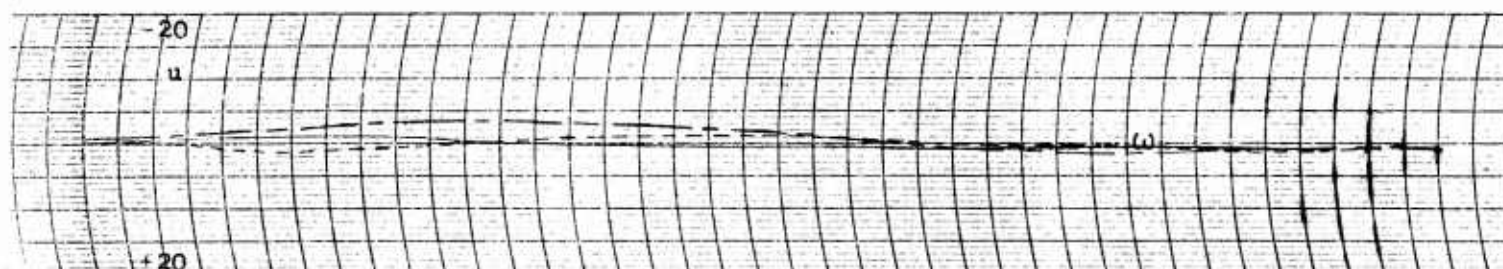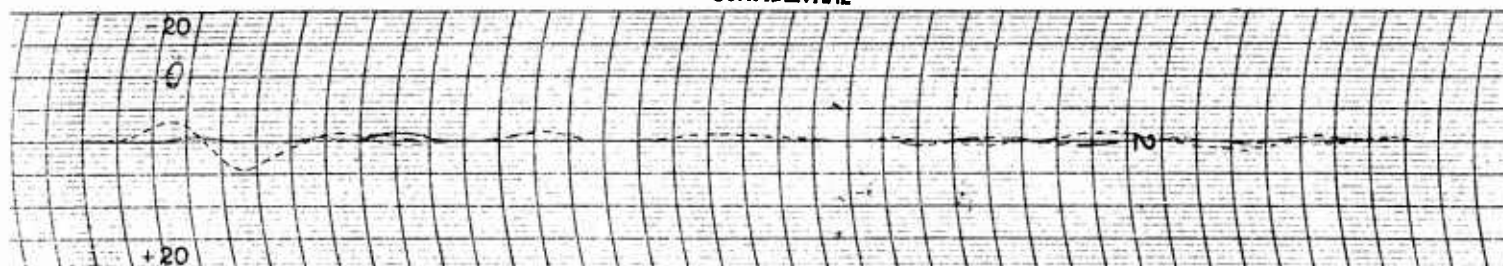
WT. = 42,390 LBS.

CONFIDENTIAL

Page 50

EFFECT OF ROLL, PITCH AND YAW GUSTS AT 30 FT./SEC. IN HOVERING

LATERAL DYNAMICS

WT. = 67,660 Lbs.

D-181-960-009

D-181-945-005

Fig. No. 7(a)

Pilot Acceptable Gradients

CONFIDENTIAL

CONFIDENTIAL

EFFECT OF ROLL, PITCH AND YAW GUSTS AT 30 FT./SEC. IN HOVERING

D-181-945-205
Fig. No. 7(b)
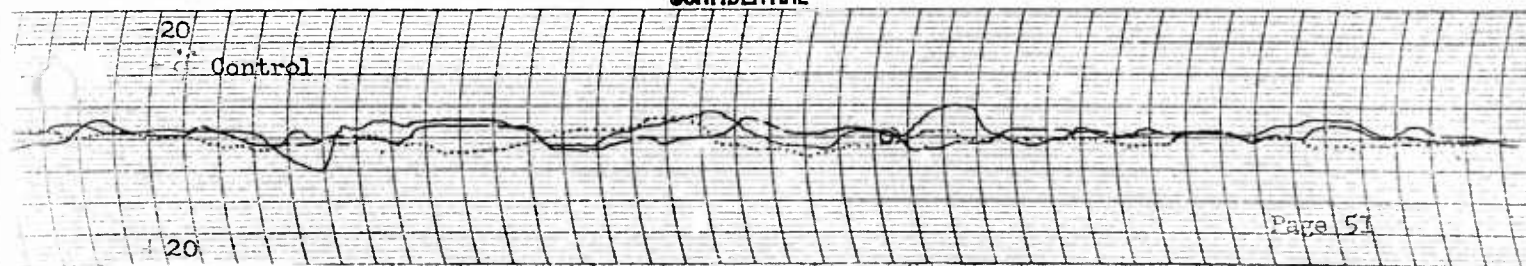
WT. = 67,660 Lbs.

LONGITUDINAL DYNAMICS

Pilot Acceptable Gradients

**CONFIDENTIAL**

$\dot{\theta}$

$u$

Roll    g
Pitch   g
Yaw    g

$v$

Gust

**CONFIDENTIAL**

Control

EFFECT OF ROLL, PITCH AND YAW GUSTS IN HOVERING
LATERAL DYNAMICS

D-181-950-009
D-181-945-005
Fig. No. 8(a)

WT. = 67,660 lbs.
Gust = 50 Ft./Sec.

Power On Duct Aerodynamics Included

CONFIDENTIAL

Roll    g
Pitch   g
Yaw     g

Gust

Control

CONFIDENTIAL

Control

Page 53
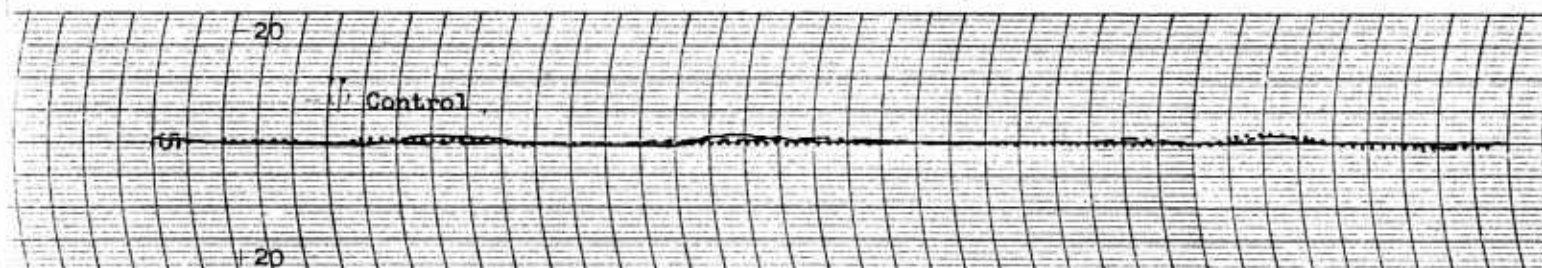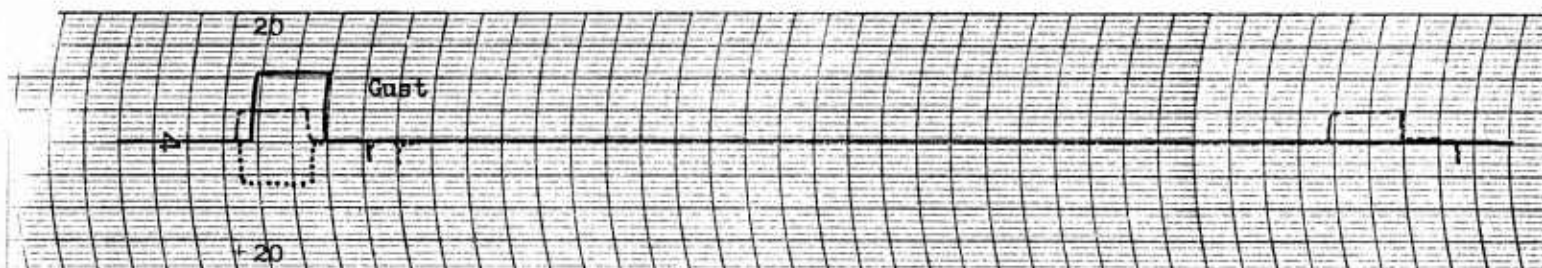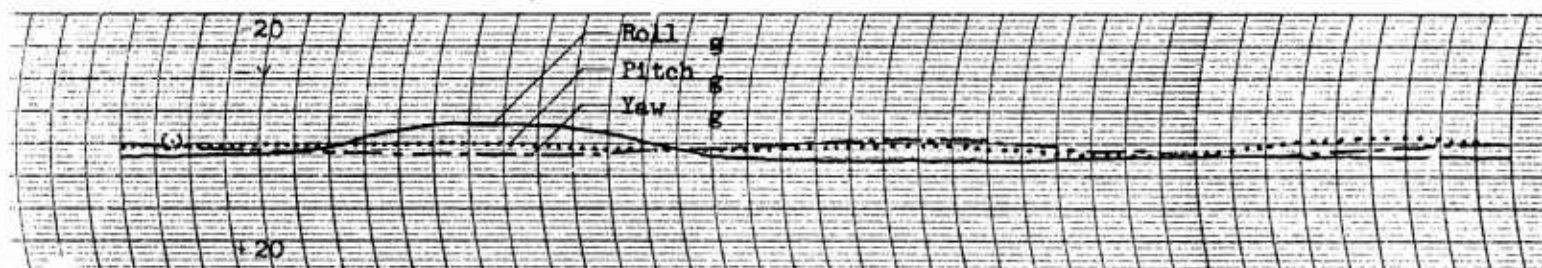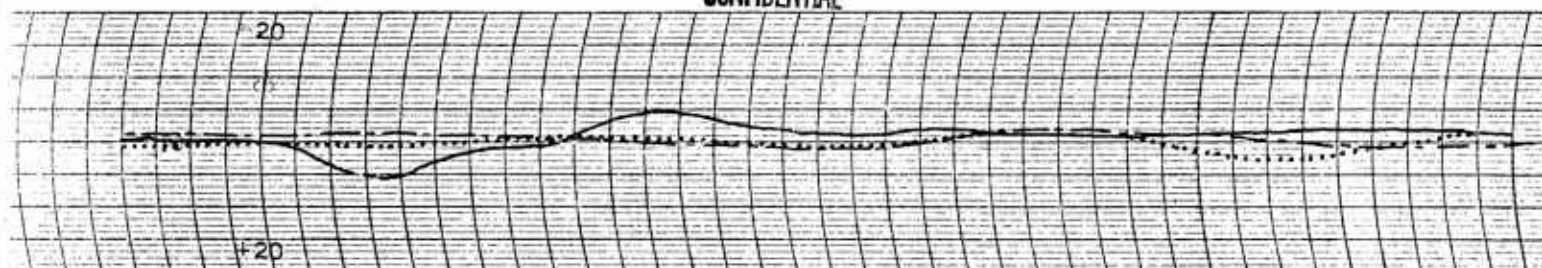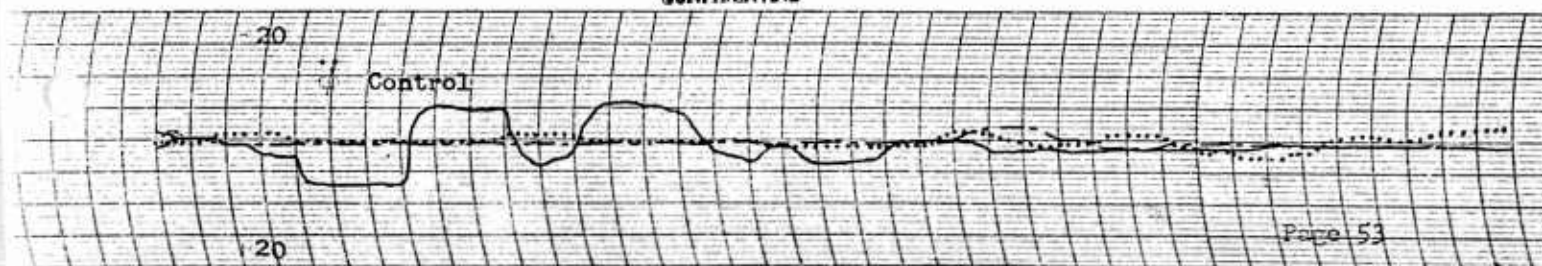
EFFECT OF ROLL, PITCH AND YAW GUST IN HOVERING

LONGITUDINAL DYNAMICS

WT. = 67,660 Lbs.

Gust = 50 Ft./Sec.

D-181-945-005
Fig. No. 8(b)

-20

+20

**CONFIDENTIAL**

-20

+20

-20

+20

Roll
Pitch
Yaw

-20

+20

-20

Gust

+20

**CONFIDENTIAL**

-20

+20

BELL *Aircraft* CORPORATION
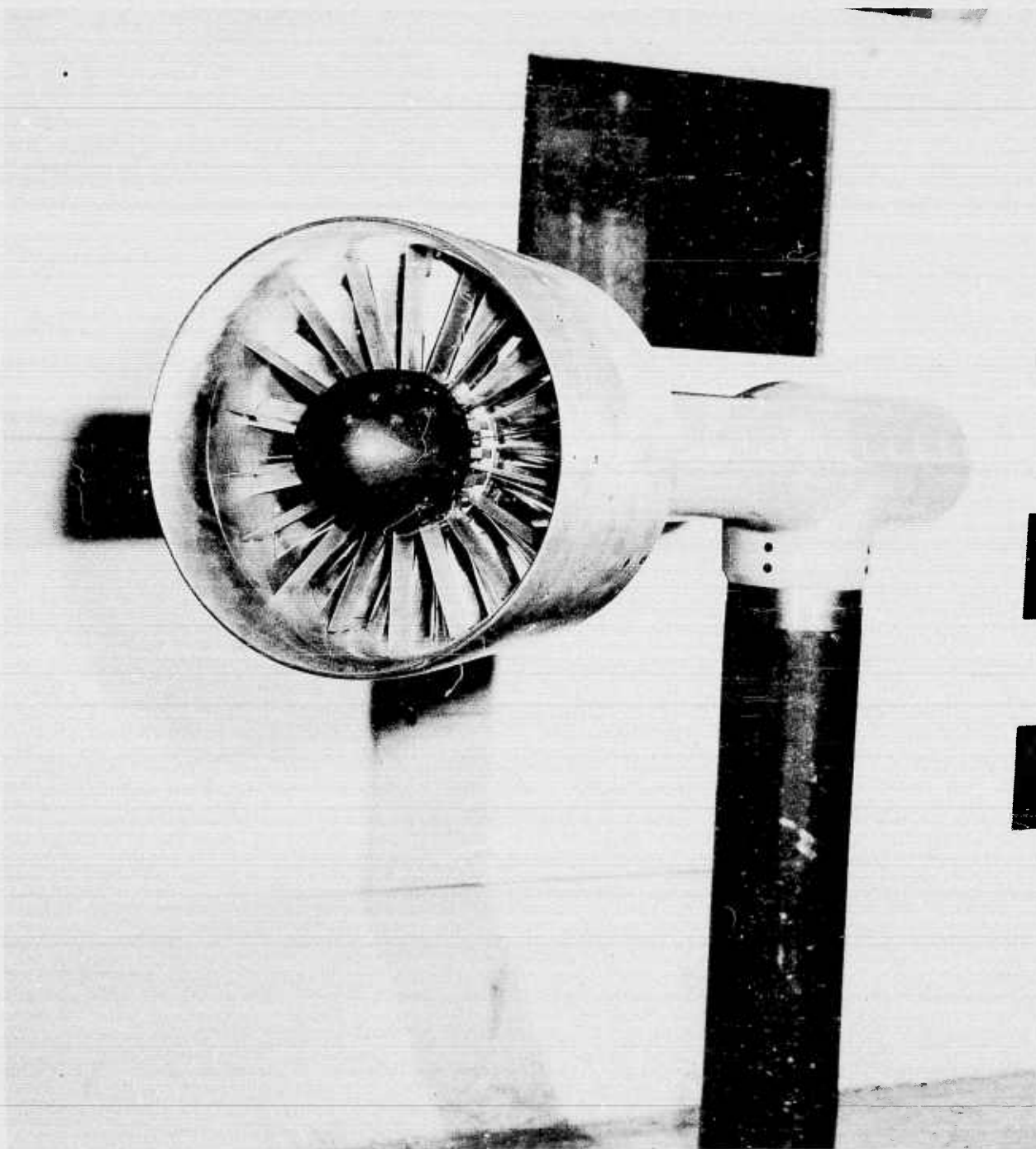


Figure 9a.  Wind Tunnel Duct Model

**BELL** *Aircraft* CORPORATION
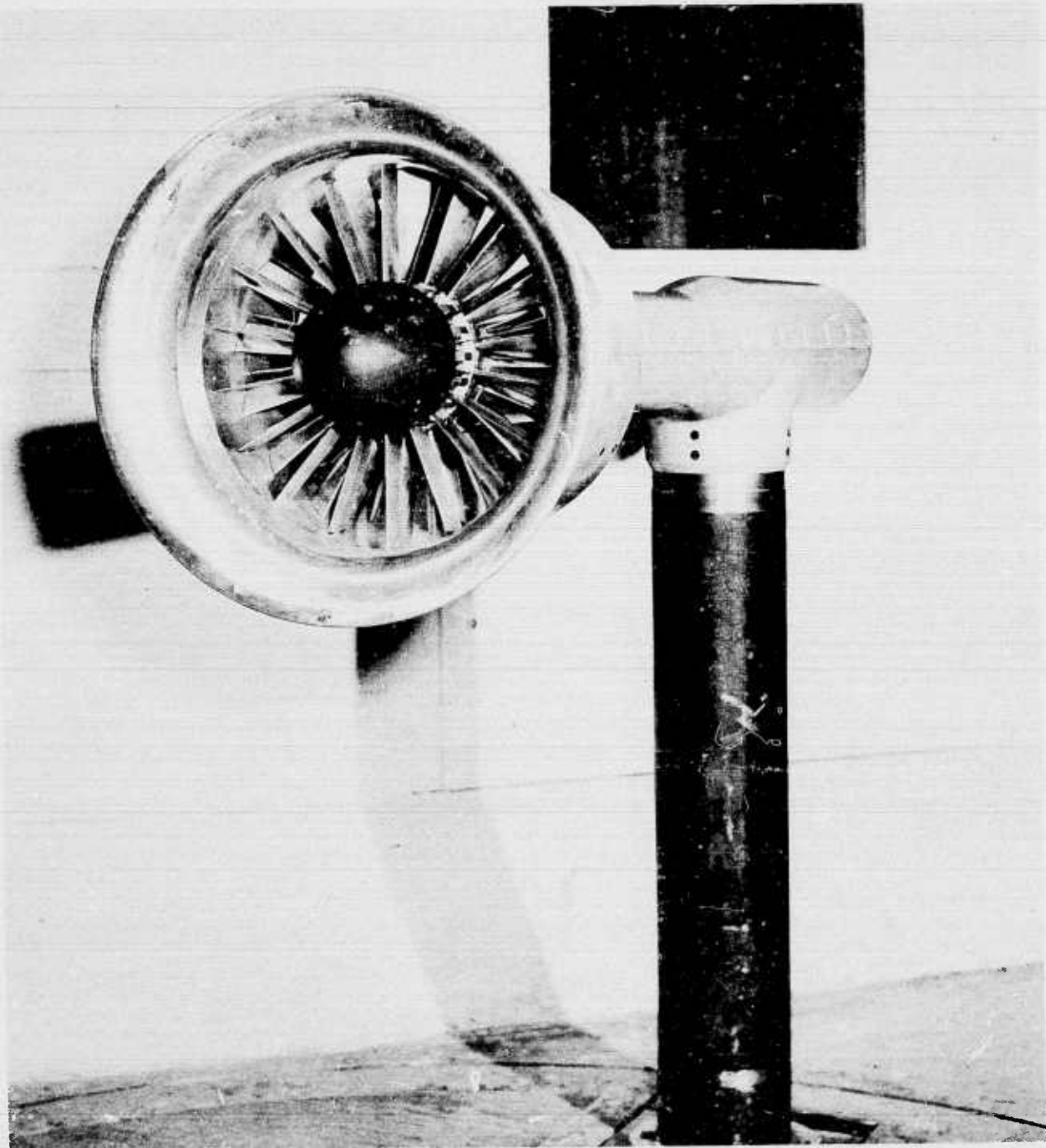


Figure 9b.  Wind Tunnel Duct Model

D-181-960-009

Fig. No. 10

## REACTION CONTROL MOMENTS REQUIRED
## IN HOVERING FOR VARIOUS GRADIENTS

$WT = 67,660^{\#}$
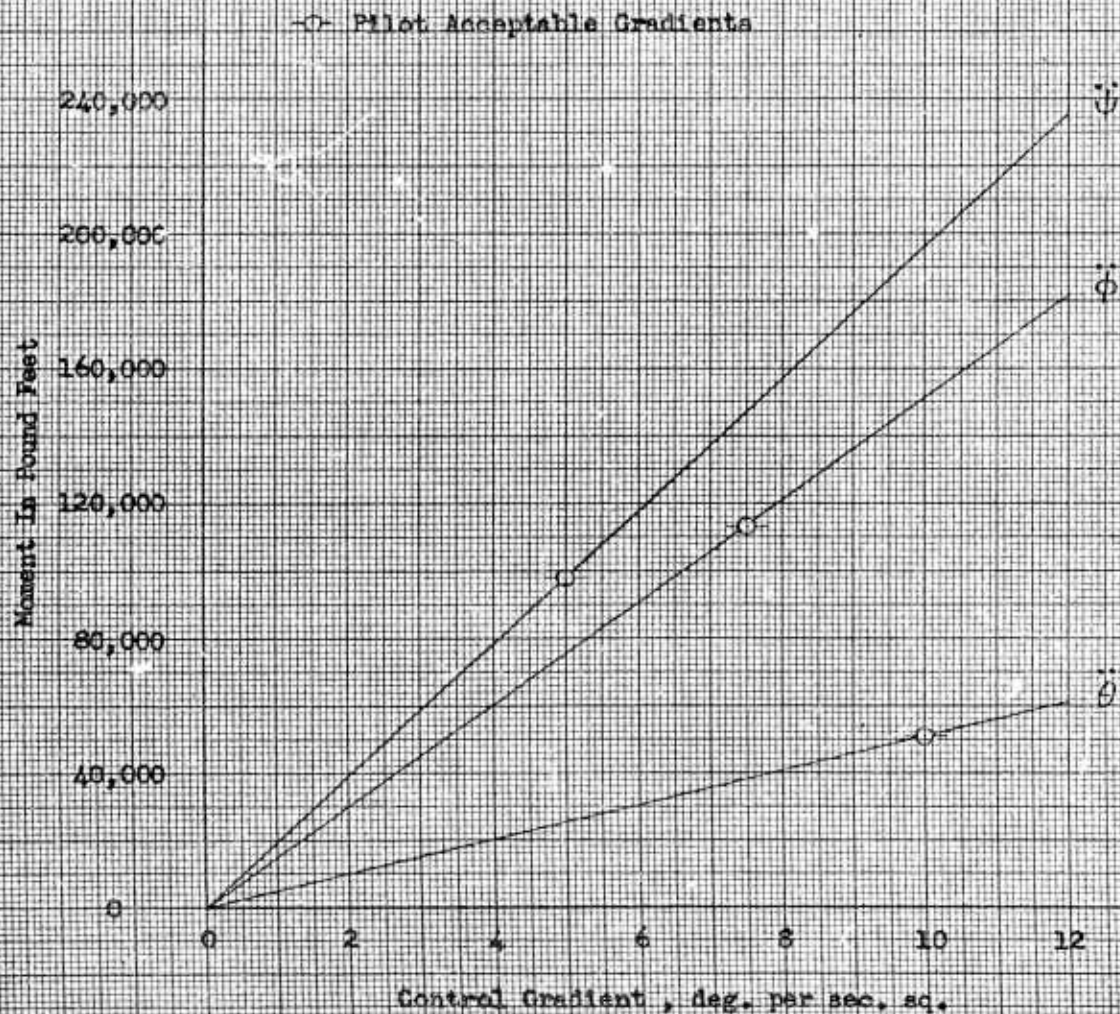


—○— Pilot Acceptable Gradients

D-181-960-009

Fig. No. 11

PITCH REACTION CONTROL FORCES AND MOMENTS
REQUIRED FOR VARIOUS PITCH GRADIENTS

Fig. No. 12(a)

Yaw Reaction Control Forces and Moments
Required for Various Yaw Gradients with
Control at Center of Outboard Wing Duct

D181-945-005

Fig. No. 12(b)

Yaw Reaction Control Forces and Moments
Required for Various Yaw Gradients With Control
at .89 (Tail) Axis
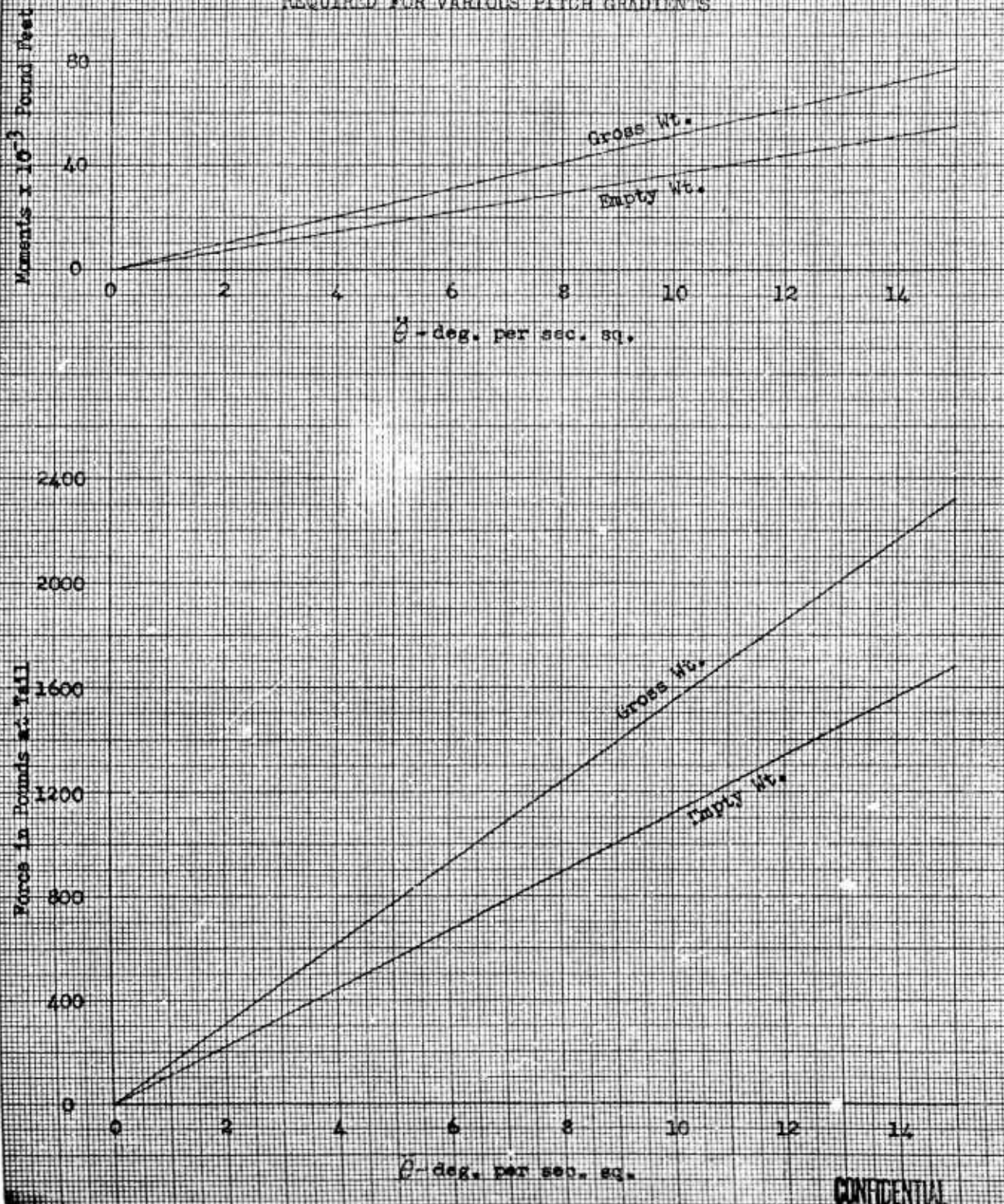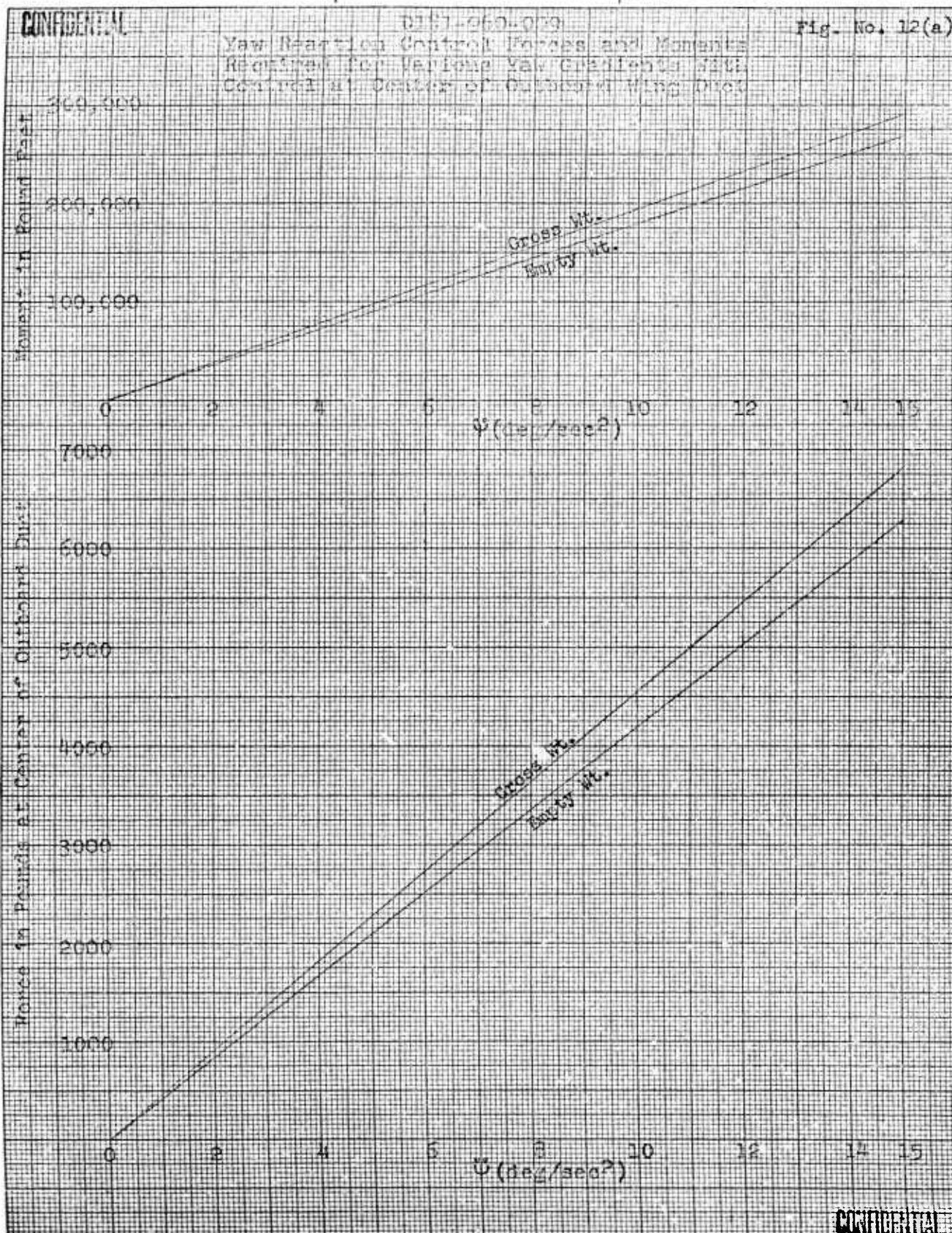
CONFIDENTIAL

D181-960-000
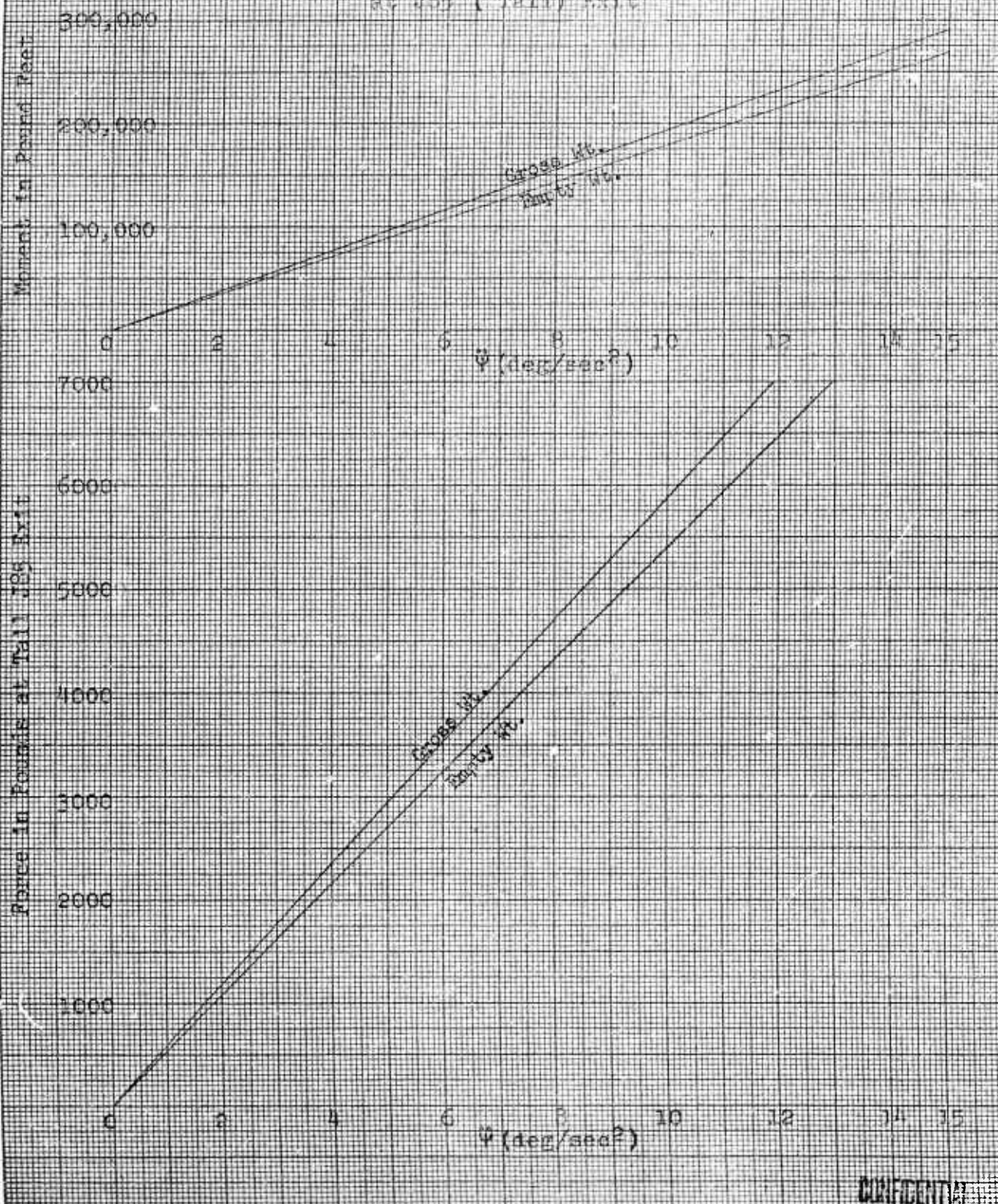
Fig. No.

### ROLL REACTION CONTROL FORCES REQUIRED FOR VARIOUS ROLL GRADIENTS REPRESENTED AS PERCENTAGE OF WEIGHT
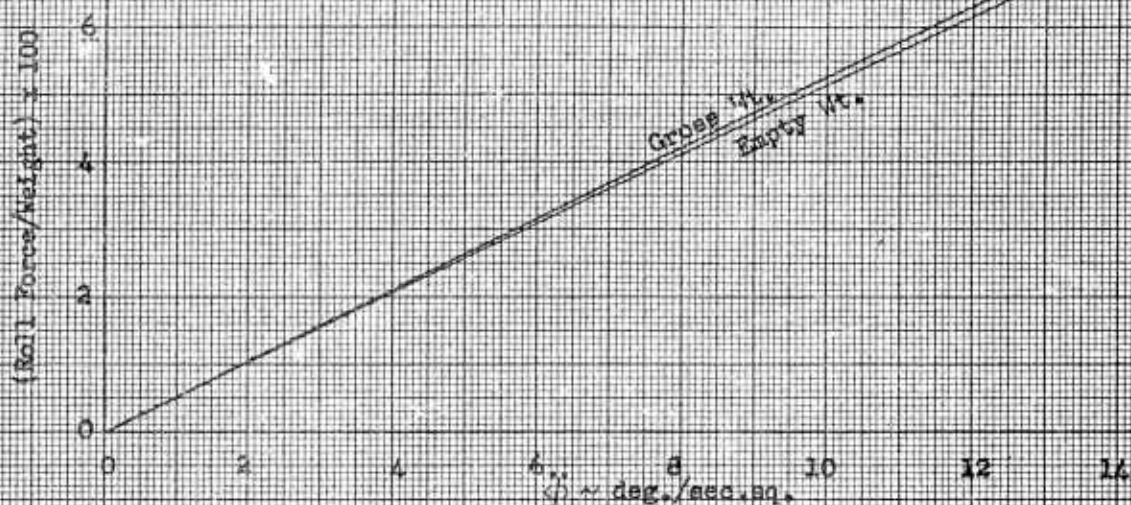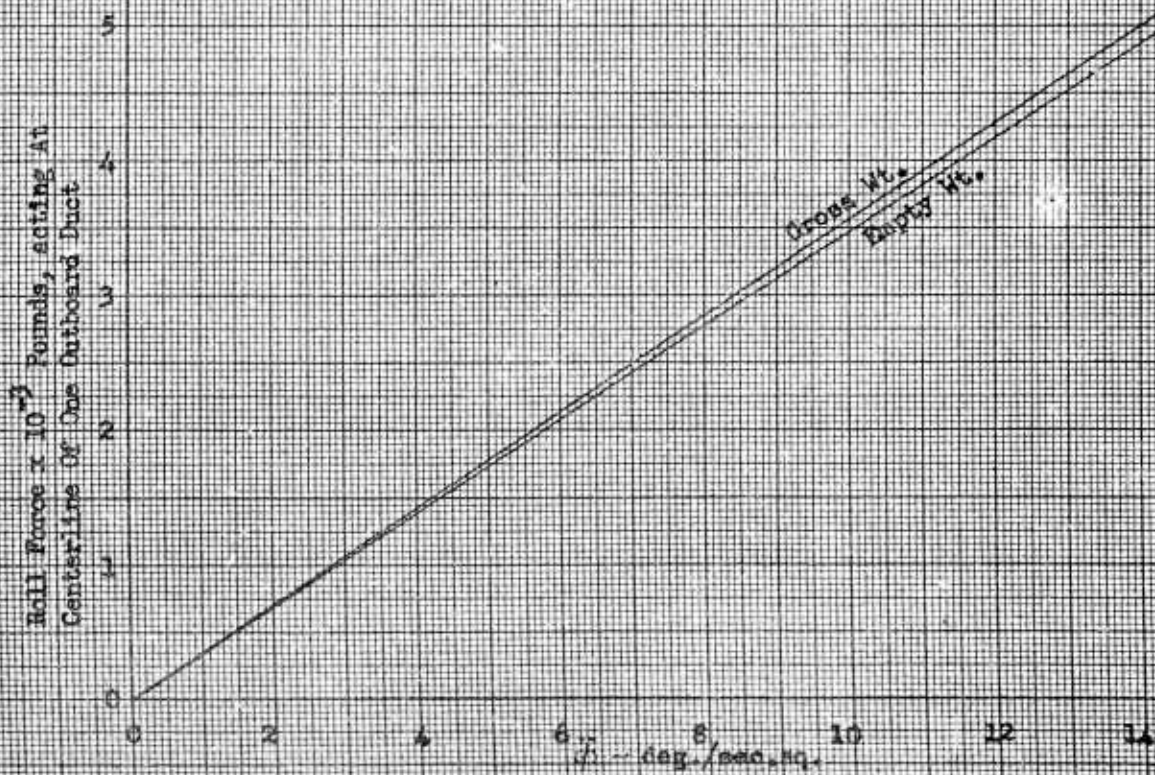


Gross Wt.

Empty Wt.

(Roll Force/Weight) x 100

$\ddot{\phi} \sim$ deg./sec.sq.

### ROLL REACTION CONTROL FORCES REQUIRED FOR VARIOUS ROLL GRADIENTS



Gross Wt.

Empty Wt.

Roll Force x $10^{-3}$ Pounds, acting At Centerline Of One Outboard Duct

$\ddot{\phi} \sim$ deg./sec.sq.

CONFIDENTIAL

CONFIDENTIAL

Fig. No. 14
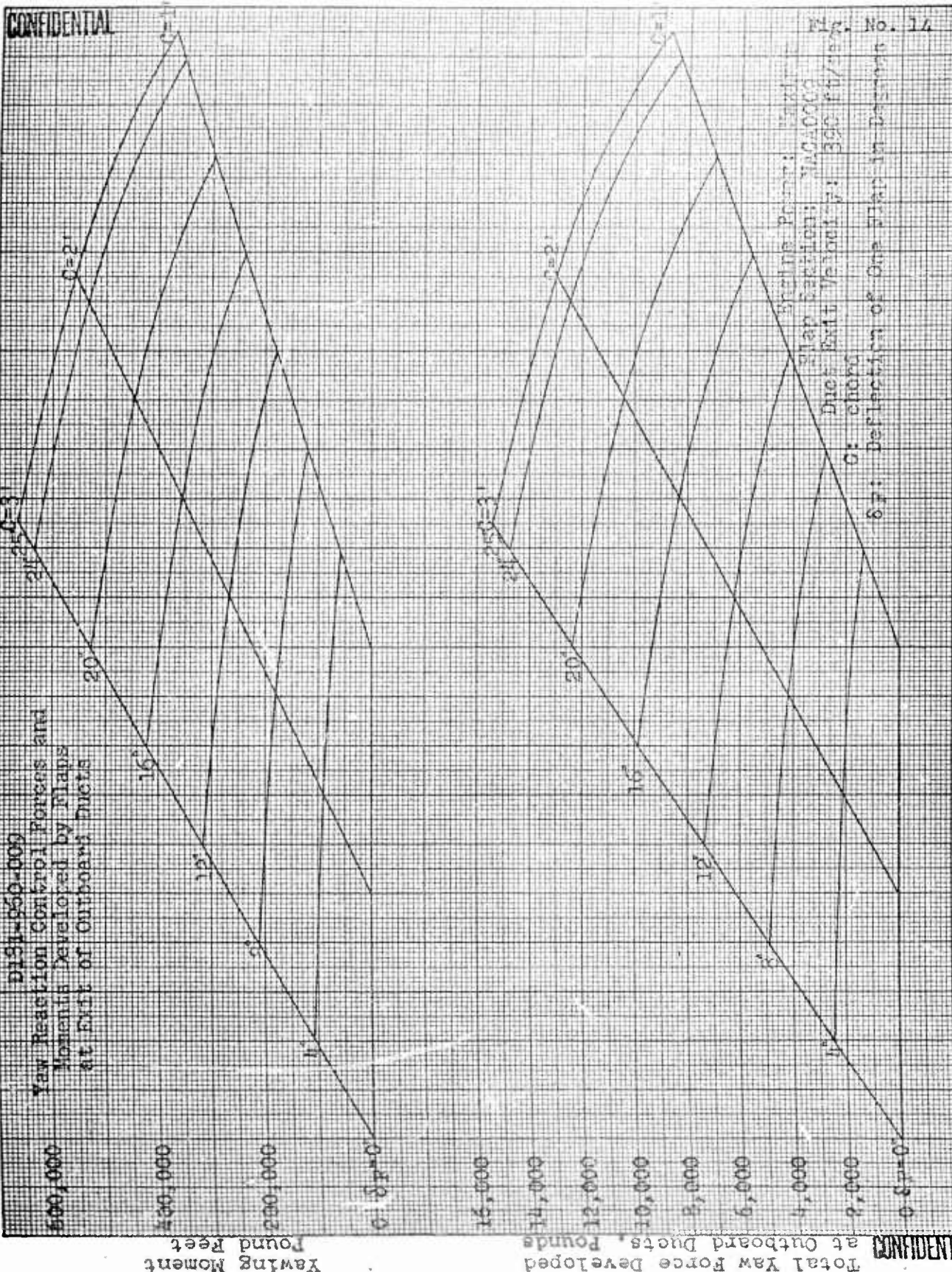
D-181-945-000

Yaw Reaction Control Forces and
Moments Developed by Flaps
at Exit of Outboard Ducts

Engine Power: Full
Flap Section: NACA0009
Duct Exit Velocity: 300 Ft/Sec
C: chord
δ: Deflection of One Flap in Degrees

δ=2°

δ=0.3

20°

16°

12°

8°

4°

0 δ=0

600,000

500,000

400,000

300,000

200,000

100,000

0 δ=0

Yawing Moment
Pound Feet

16,000

14,000

12,000

10,000

8,000

6,000

4,000

2,000

0 δ=0

Total Yaw Force Developed
at Outboard Ducts, Pounds

CONFIDENTIAL

Roll Reaction Control Forces
Developed by Split Flap at
Exit of One Outboard Duct

Fig. No. 15

Data:
 Thrust, Static: 50,000 lbs.
 % Maximum Power: 55%
 Duct Exit Velocity: 305'/sec.
 C: Chord
 Y: Included Angle
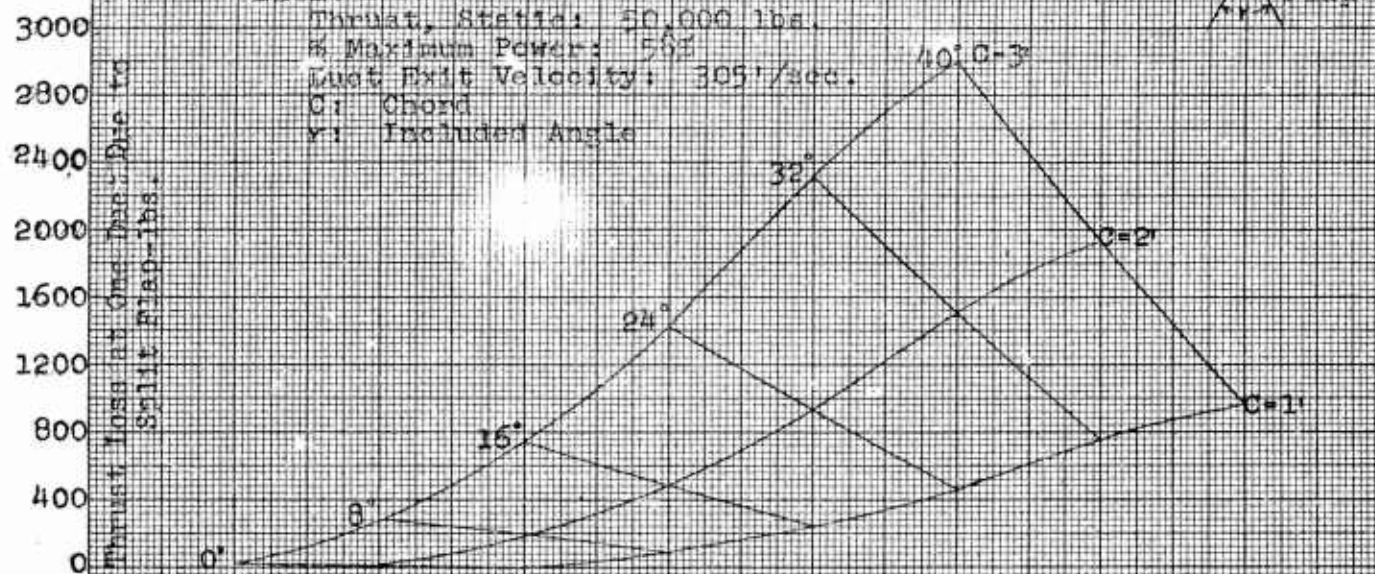
Data:
 Thrust: 72,100 lbs.
 Power: Maximum
 Duct Exit Velocity: 390'/sec.
 C: Chord
 Y: Included Angle
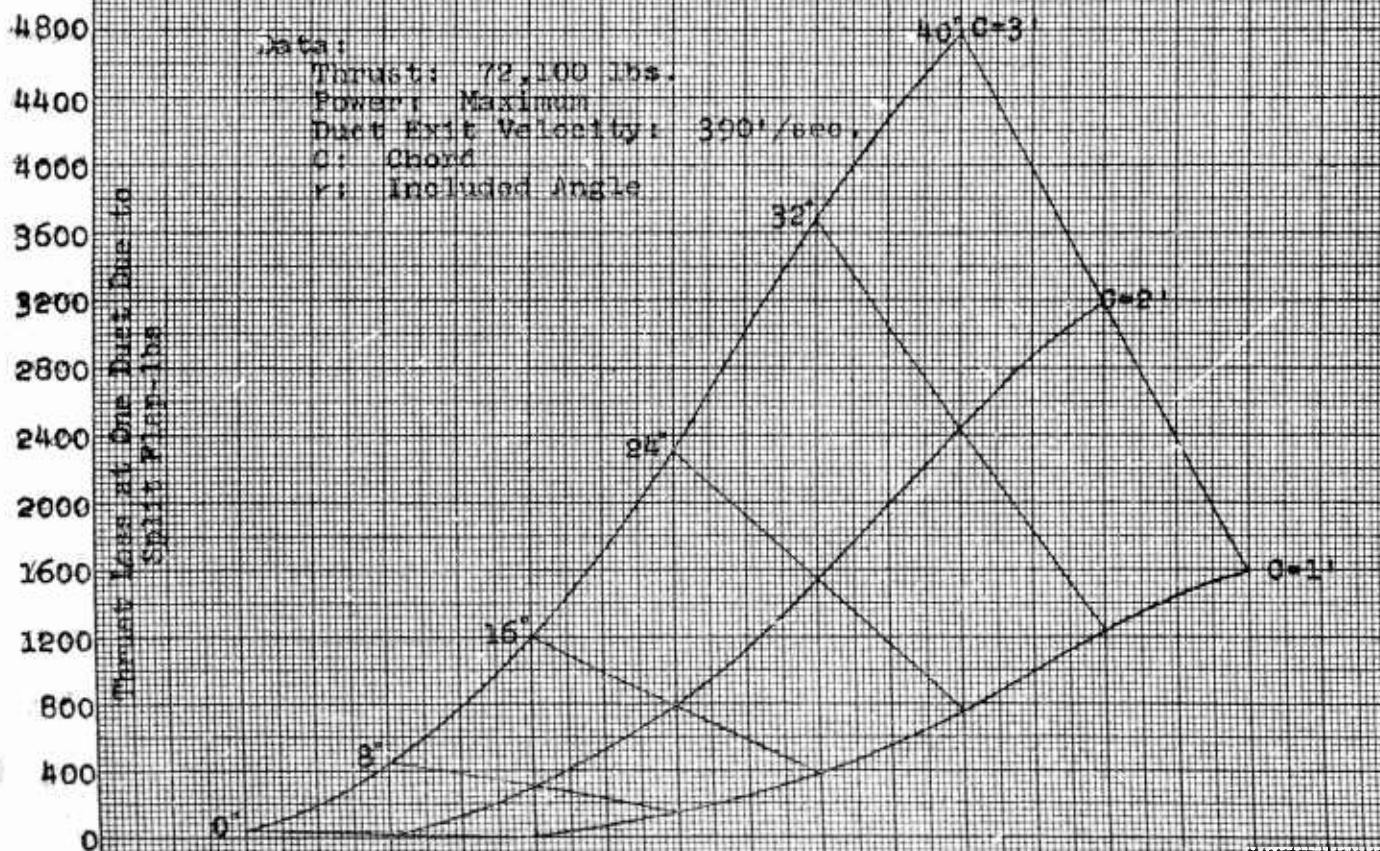
TRANSITION LATERAL TRACES

$\psi$

$Wt. = 67,660$ lbs.     Roll Gust $= 8.6°/sec^2 = 50!/sec$

REACTION CONTROL:                    **CONFIDENTIAL**     PROBLEM CONDITIONS:

$\ddot{\phi} = 7.5°/sec^2$                                   $V_o = 170.8'/sec$

$\ddot{\theta} = 10.0°/sec^2$                                   $\phi =$

$\ddot{\psi} = 5.0°/sec^2$                                   $\Lambda = 50°$

$\beta$                                                         $T = 67,060$ lbs.

$\phi$

$\ddot{\phi}$ control

$\ddot{\psi}$ control

**CONFIDENTIAL**

Gust

TECHNICAL CHARTS INCORPORATED, BUFFALO, N.Y.
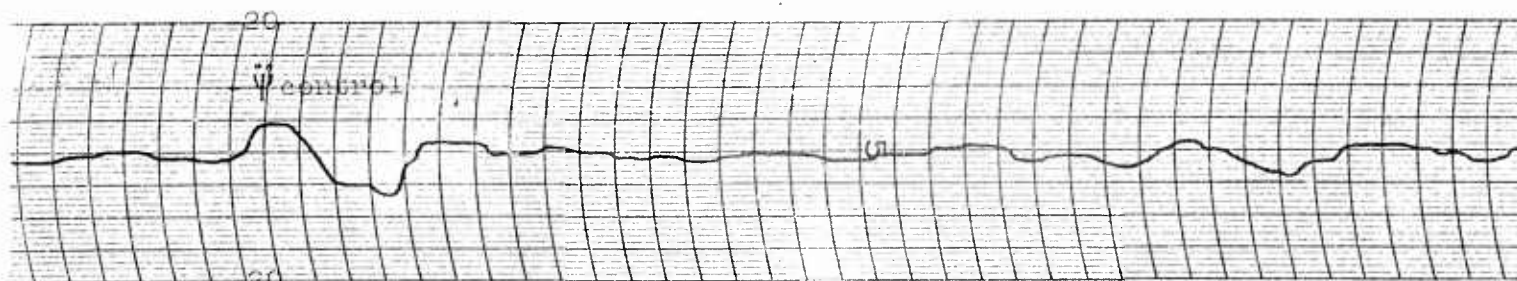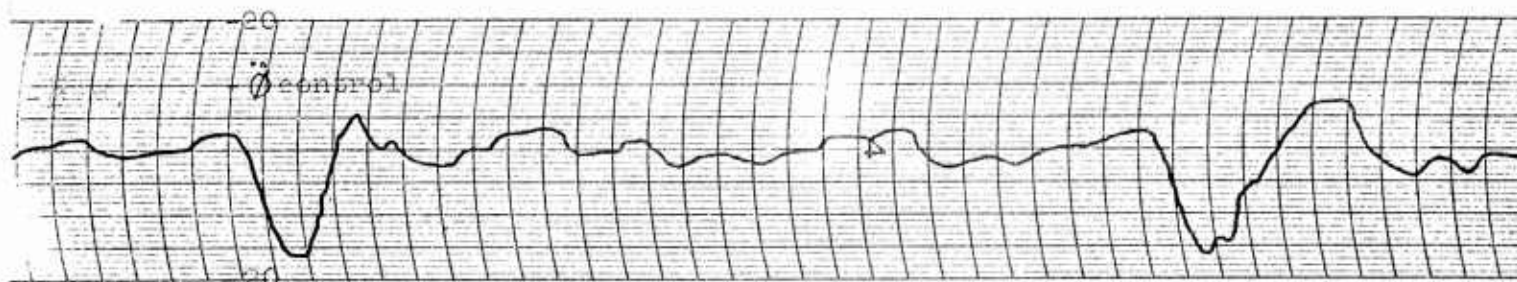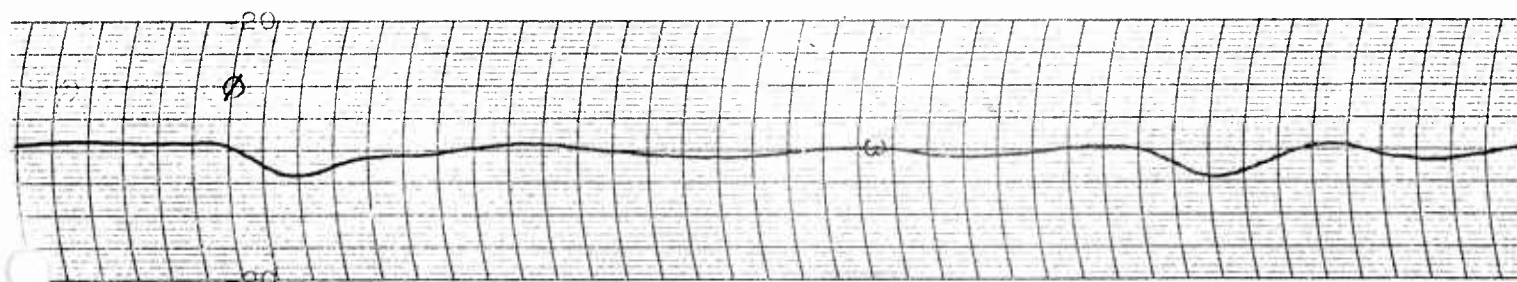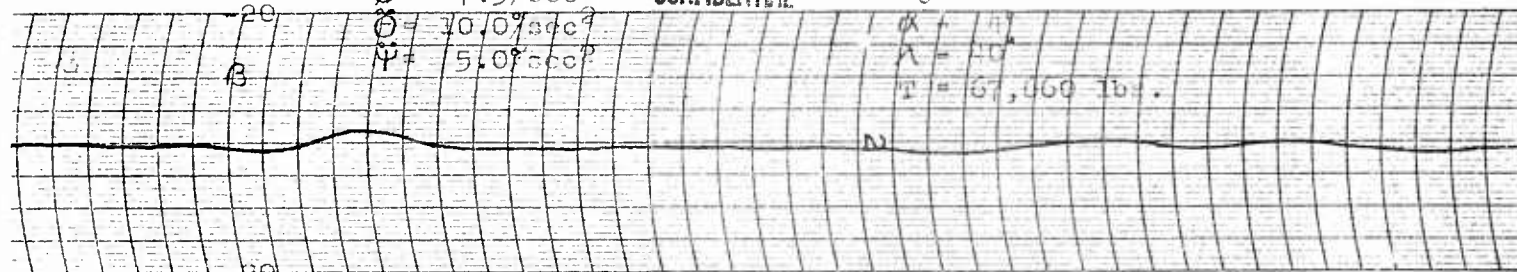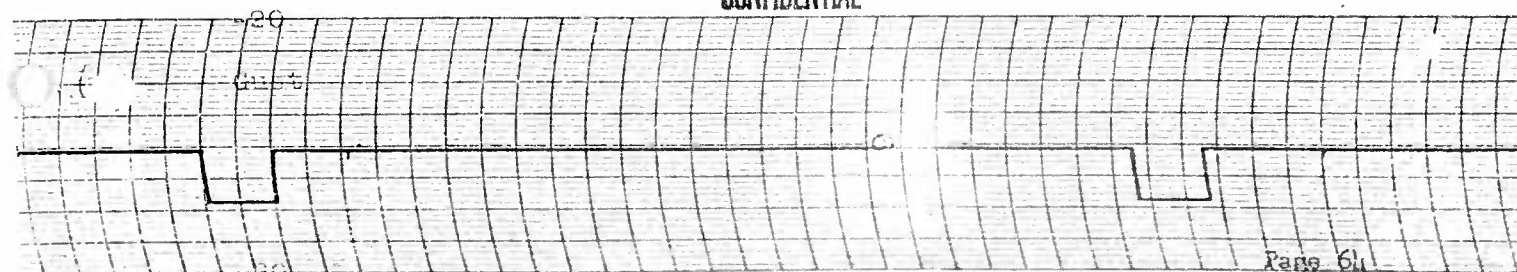
TRANSITION LONGITUDINAL TRACES

Wt. = 67,560 lbs.    Roll Gust = 5.0°/sec² = 50°/sec

REACTION CONTROL:                    PROBLEM CONDITIONS:
    Φ = 7.5°/sec²          **CONFIDENTIAL**        $V_o$ = 170.8'/sec
    Θ = 10.0°/sec²                                 α =
    Ψ = 5.0°/sec                                   γ =
                                                   T = 67,560 lbs.

**CONFIDENTIAL**

TRANSITION LATERAL TRACES

Wt. = 67,660 lbs.    Pitch Gust = 5.35°/sec², 50'/sec

REACTION CONTROL:                    PROBLEM CONDITIONS:
$\ddot{\phi} = 7.5$/sec²                     $V_0 = 170.8'$/sec
$\ddot{\theta} = 10.0$°/sec²                  $\alpha = 4°$
$\ddot{\psi} = 5.10$/sec²                     $\lambda = 40°$
                                     $T = 67,660$ lbs.

CONFIDENTIAL

TRANSITION LONGITUDINAL TRACES

t. = 67,660 lbs.    Pitch Gust = 5.35°/sec² = 50°/sec

REACTION CONTROLS:                PROBLEM CONDITIONS:

$\ddot{\phi}$ = 7.5°/sec²           $V_0$ = 170.6°/sec

$\ddot{\theta}$ = 10.0°/sec²        $\alpha$ = 4°

$\ddot{\psi}$ = 5.0°/sec²           $\lambda$ = 40°

**CONFIDENTIAL**                    T = 57,660 lbs.

$\theta$

$\alpha$

$\frac{\Delta V}{V}$

gust

**CONFIDENTIAL**

$\dot{\theta}$ control

TRANSITION LATERAL TRACES

Wt. = 67,660 lbs. Yaw gust = 1°/sec² = 50°/sec

REACTION CONTROL: PROBLEM CONDITIONS:
$\ddot\phi = 7.5°/\sec^2$ $V_o = 170.8'/sec$
$\ddot\theta = 10.0°/\sec^2$
$\ddot\psi = 5.0°/\sec^2$ $\lambda = 40°$
$= 67,660$ lbs.

CONFIDENTIAL

CONFIDENTIAL

D-181-960-009                    D-181-945-005
                                  Fig. No. 21

TRANSITION LONGITUDINAL TRACES

WT.=67,660 lbs.        Yaw Gust=1°/sec²=50'/sec

REACTION CONTROL:              PROBLEM CONDITIONS:
$\dot{\phi} = 7.5°/sec^2$        $V_0 = 170.0'/sec$
$\dot{\theta} = 10.0°/sec^2$     $\alpha = 4°$
$\ddot{\psi} = 5.0°/sec^2$       $\lambda = 40°$
                                  T = 67,650 lbs.
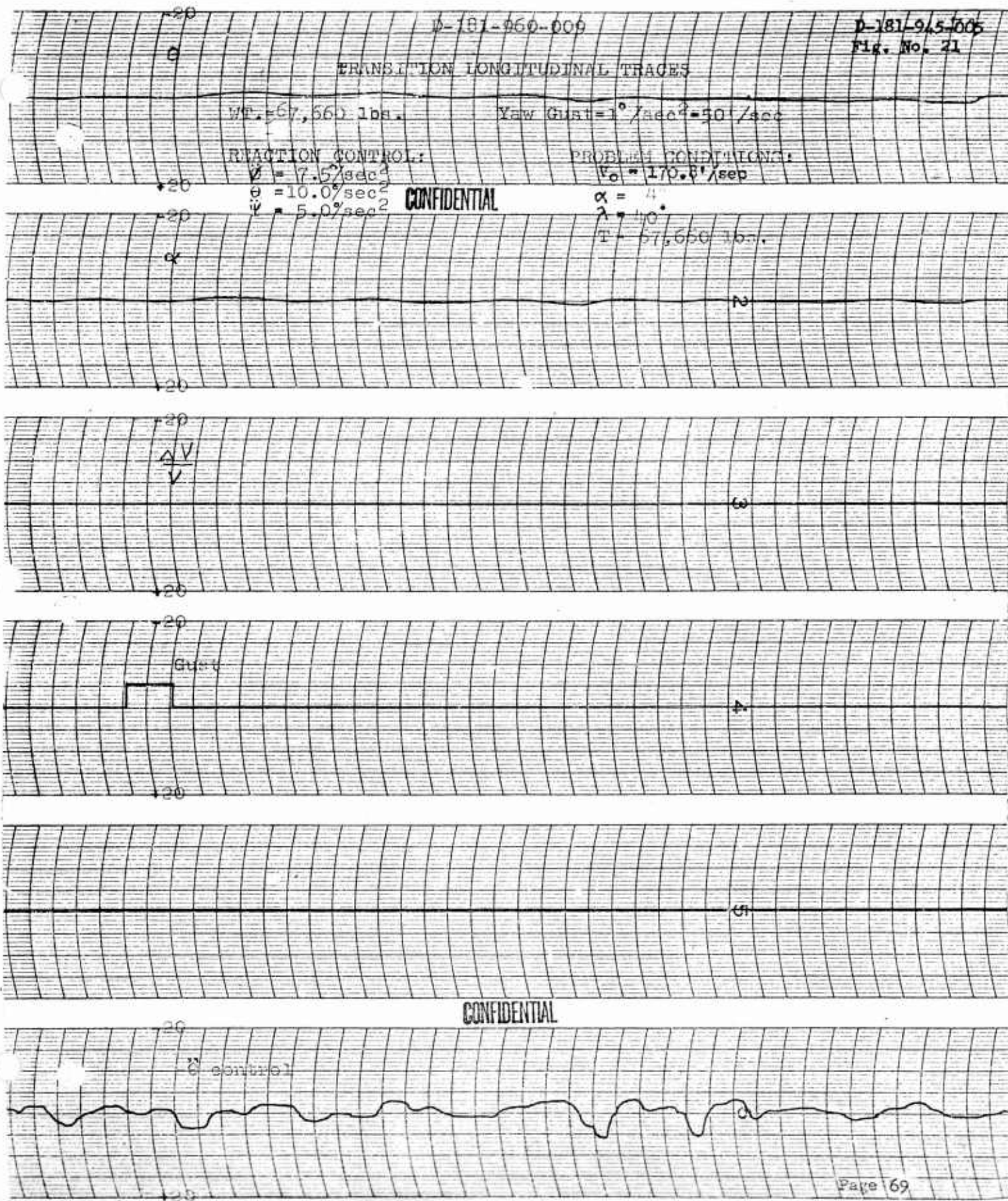
CONFIDENTIAL

CONFIDENTIAL

CONFIDENTIAL

Fig. No. 22

D-181-960-009

HORIZONTAL TAIL PANEL
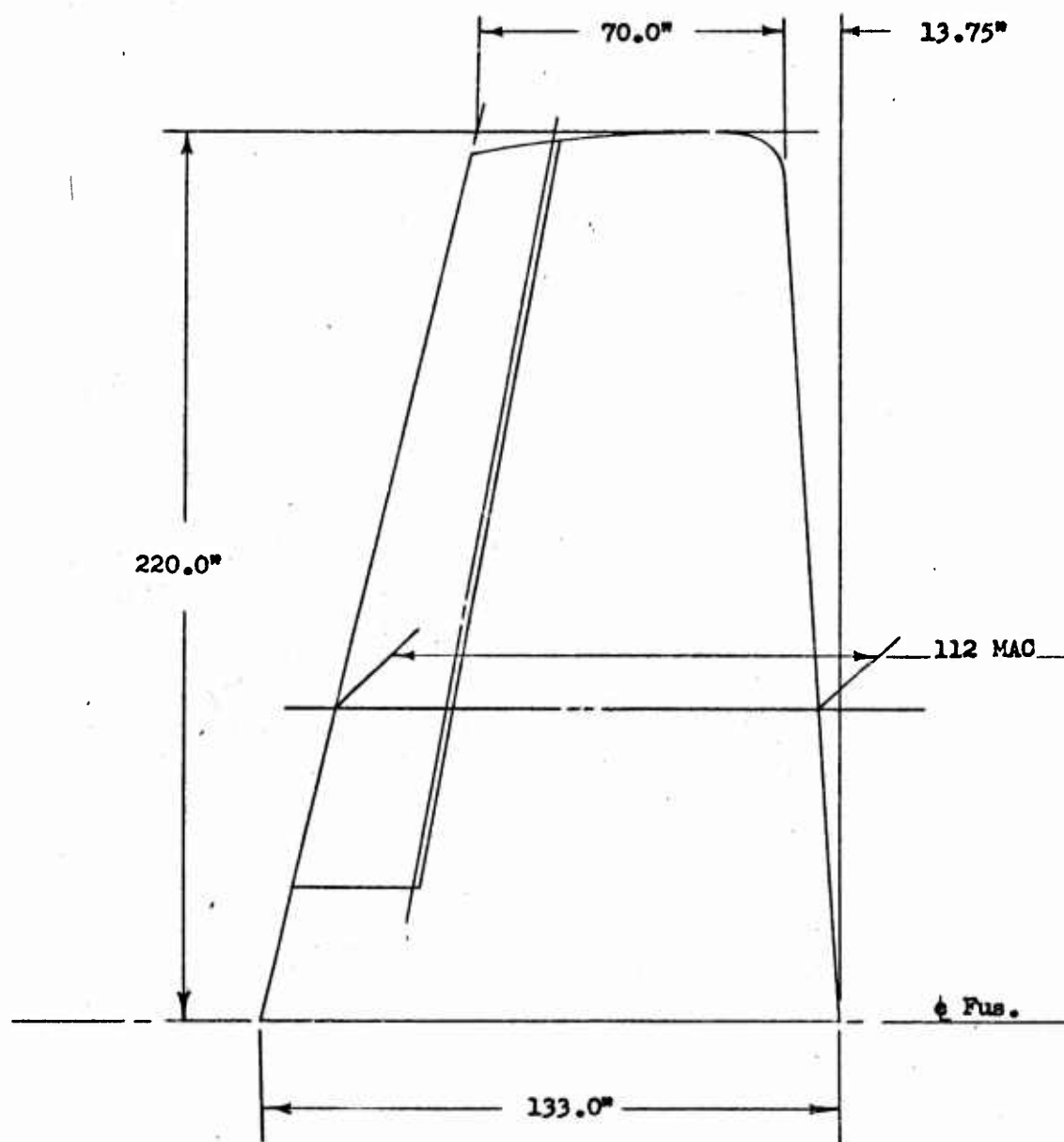


CONFIDENTIAL

Form E4-1 Rev. 353

Fig. No. 23

D-181-960-009

LIFT CURVE SLOPES
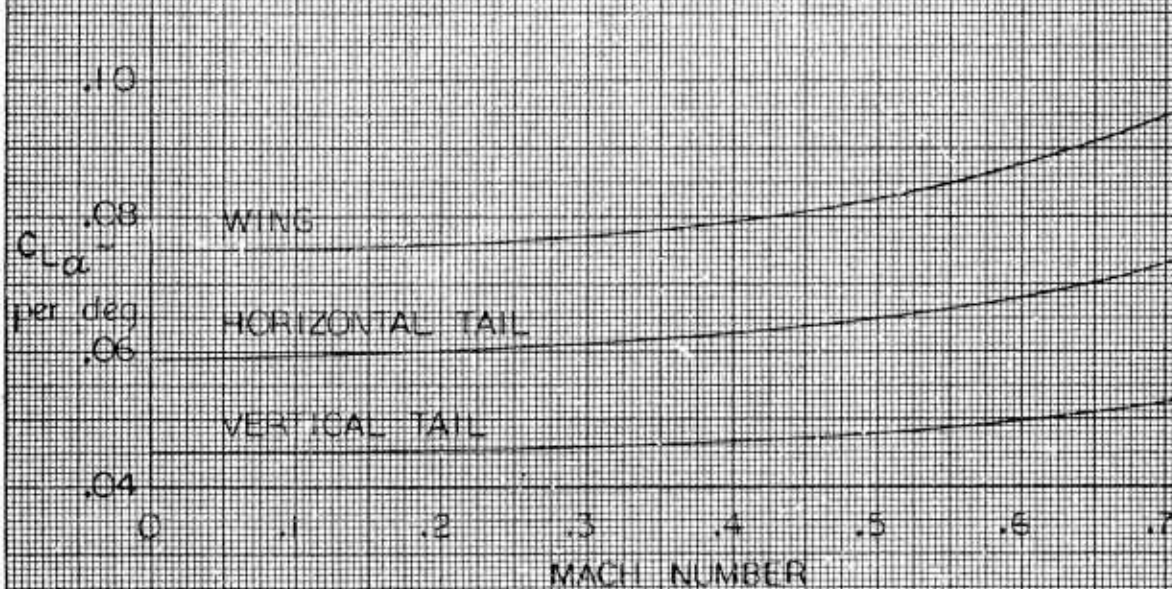
Fig. No. 24



SIDE VIEW OF INBOARD AND OUTBOARD DUCT

STA-30

Outboard Duct

Inboard Duct

157.0"

116.0"

147.0"

114.0"

Fig. No. 25

D-181-930-009

LONGITUDINAL STABILITY COMPONENTS
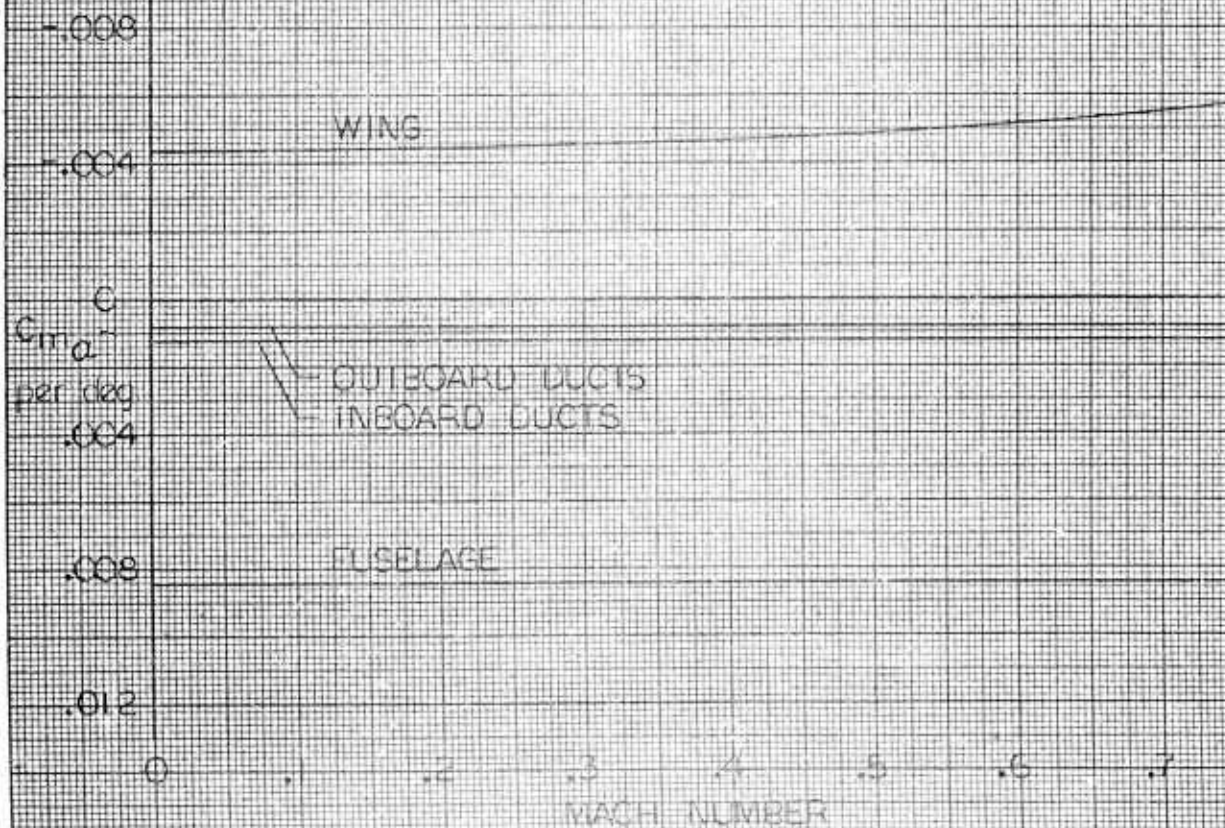
WING

$C_{m_\alpha} = \frac{C}{\alpha}$ per deg

OUTBOARD DUCTS
INBOARD DUCTS

FUSELAGE

MACH NUMBER

FIG. No. 26

D-181-960-009

CHANGE OF AERODYNAMIC ANGLE OF ATTACK OF HORIZONTAL TAIL
WITH WING ANGLE OF ATTACK
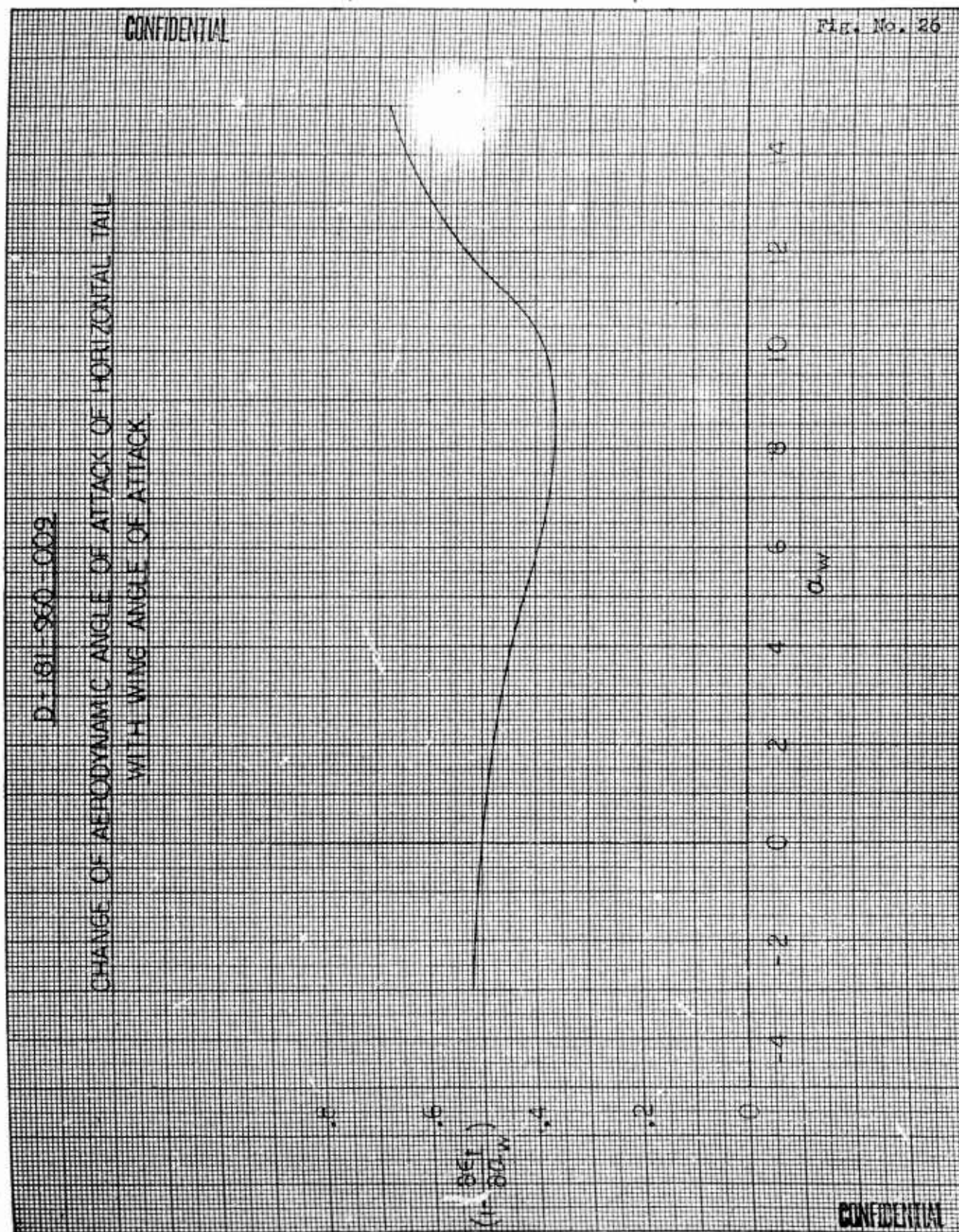
CONFIDENTIAL

Fig. No. 27



PITCHING MOMENT DUE TO ANGLE OF ATTACK OF THE HORIZONTAL TAIL

D-181-960-009

$(C_{m_\alpha})_{HT} = f(C_L, M)$

Fig. No. 28

AIRPLANE LONGITUDINAL STABILITY
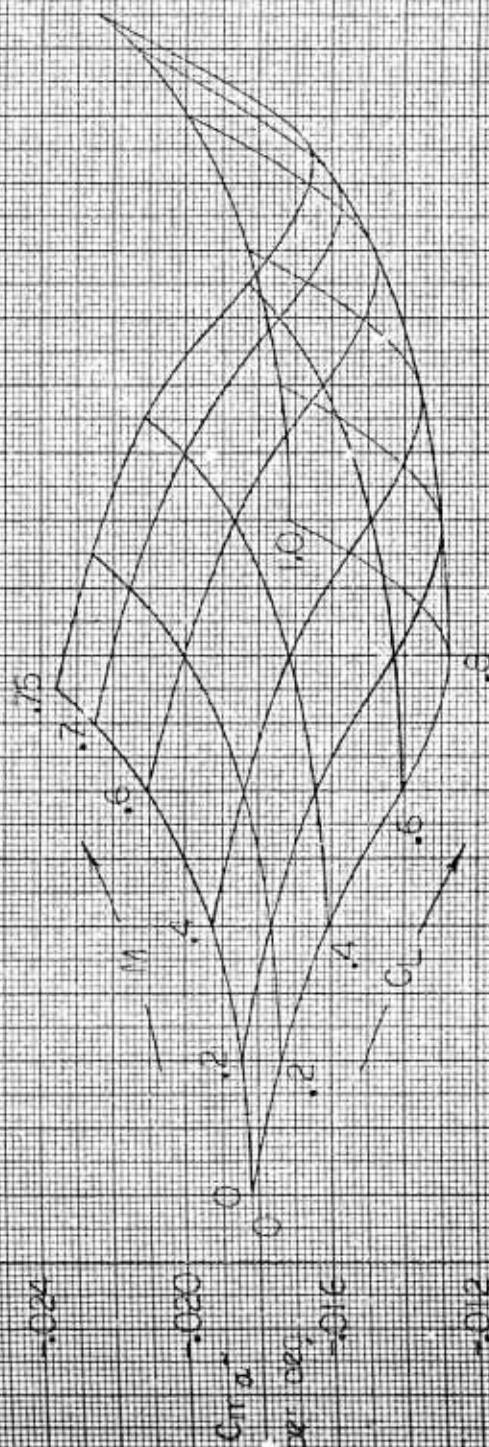
D-181-960-009

CONFIDENTIAL

Fig. No. 29

D-181-960-009

AIRPLANE LONGITUDINAL STABILITY
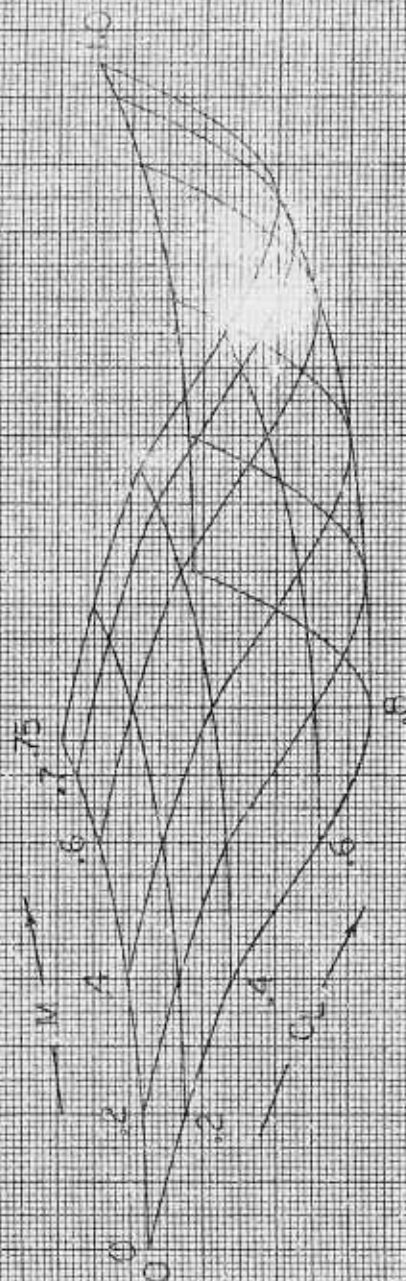
CONFIDENTIAL

Fig. No. 30

D-181-960-009

VERTICAL TAIL



CONFIDENTIAL

CONFIDENTIAL

D-181-900-009
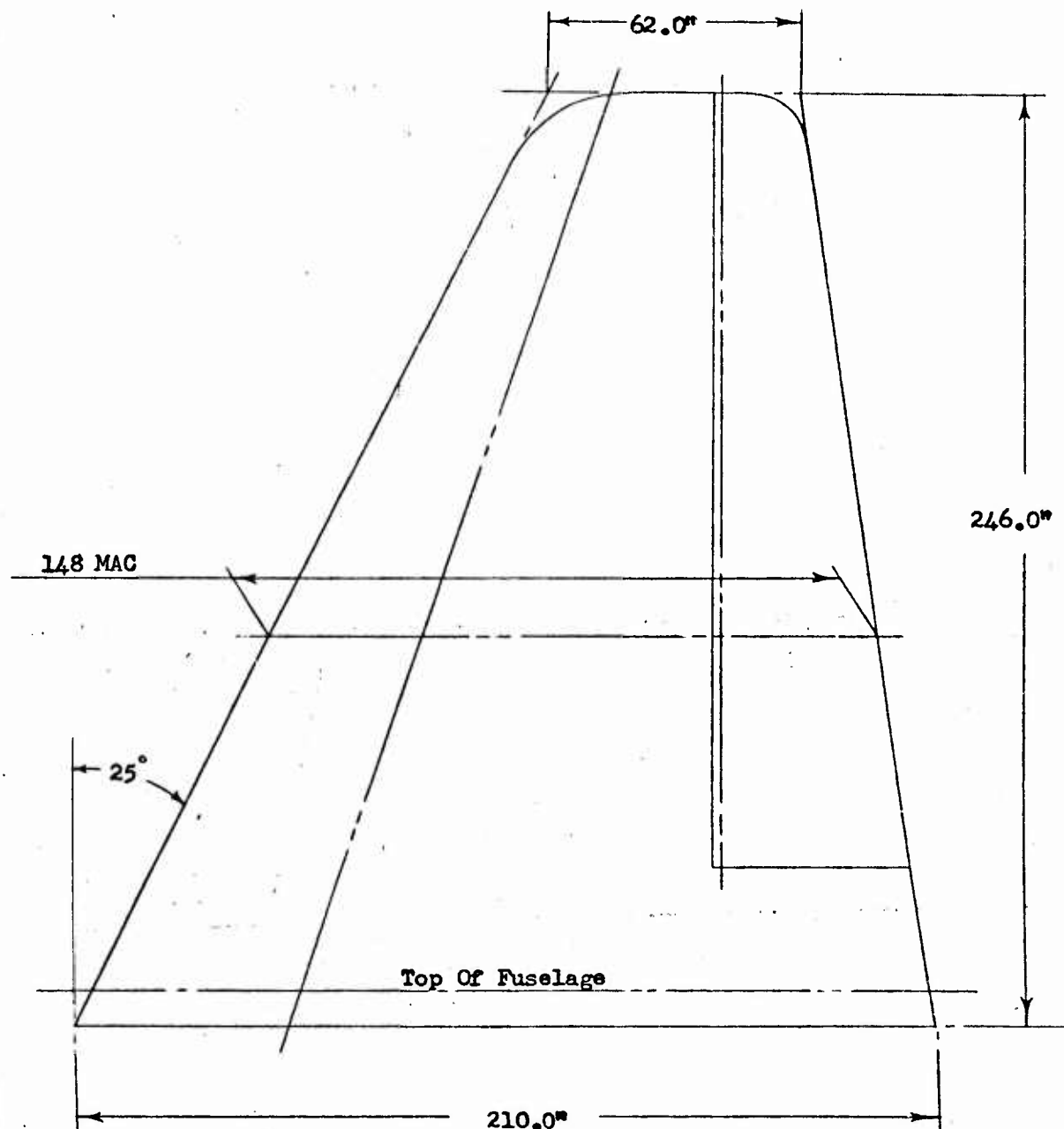
Fig. No. 31

VARIATION OF SIDE FORCE DUE TO SIDESLIP OF VERTICAL
TAIL WITH MACH NUMBER
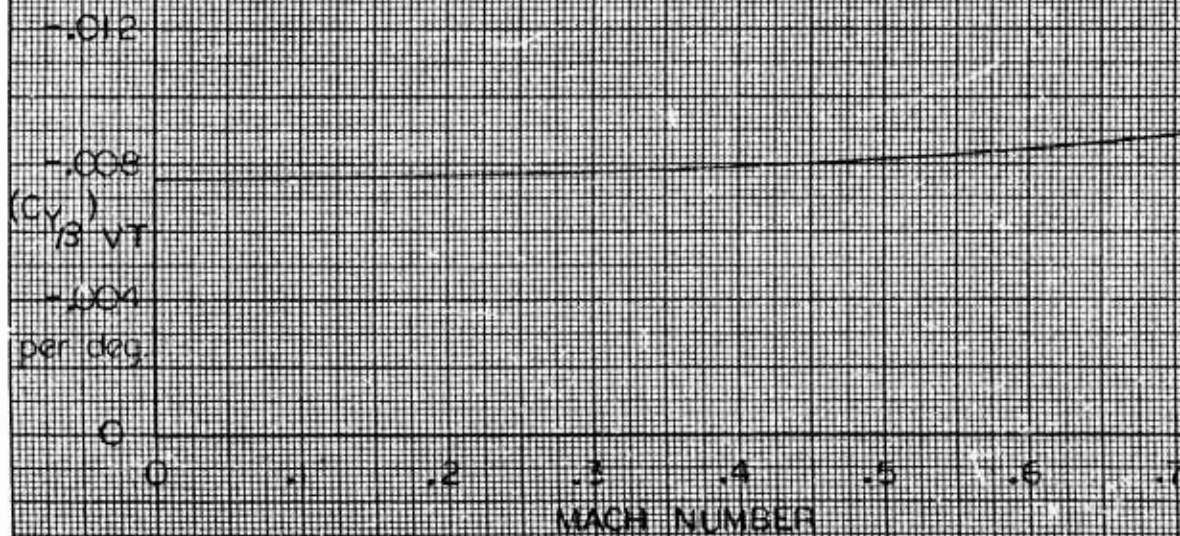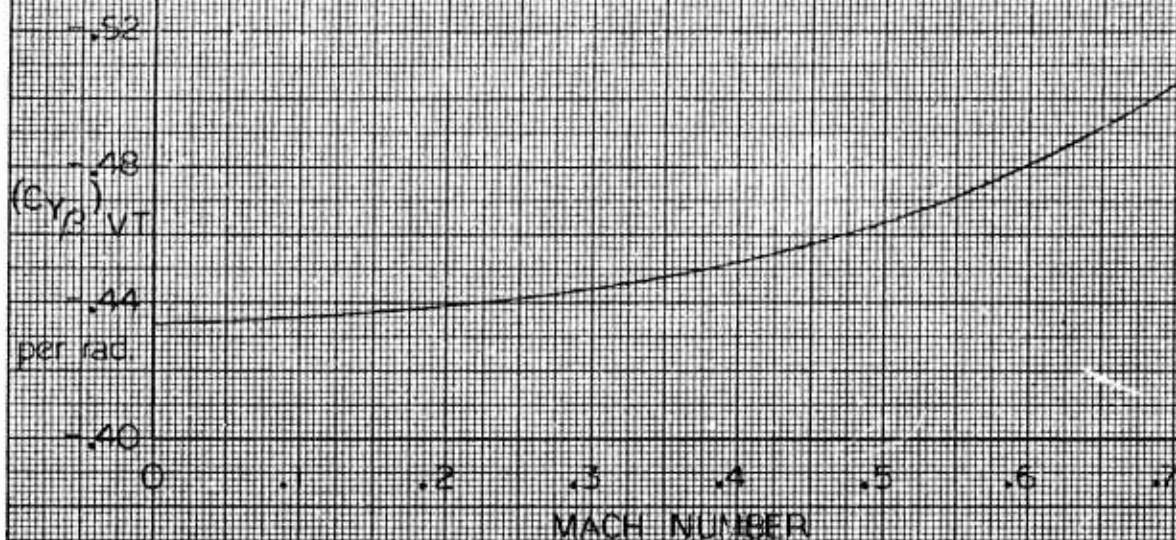
$(C_{Y_\beta})_{VT}$ per rad

MACH NUMBER

$(C_{Y_\beta})_{VT}$ per deg.

MACH NUMBER

CONFIDENTIAL

CONFIDENTIAL

D-181-945-005

DIRECTIONAL STABILITY CONTRIBUTION COMPONENTS
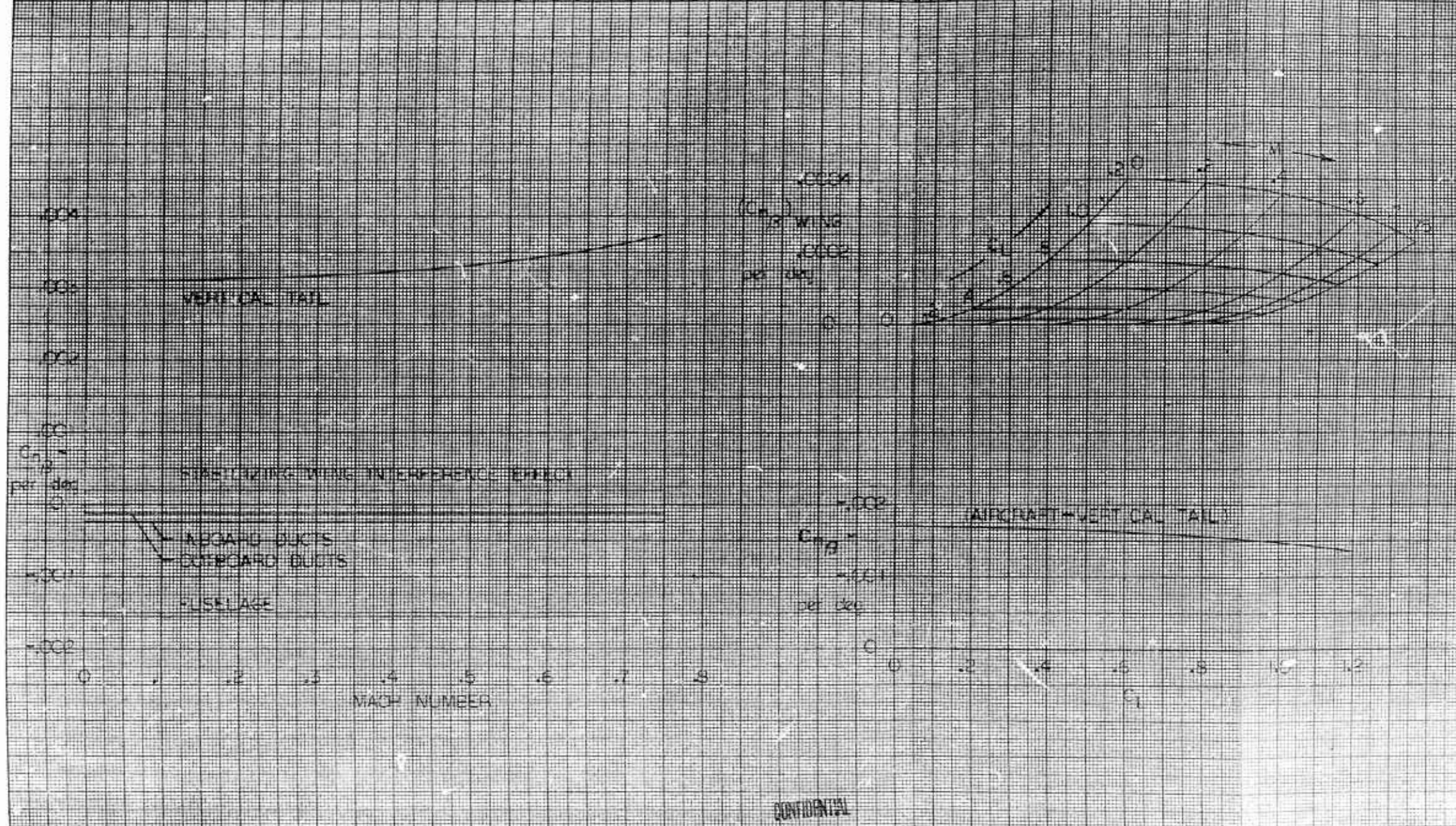


VERTICAL TAIL

$(C_{n_\beta})$ WING

per deg

STABILIZING WING INTERFERENCE EFFECT

INBOARD DUCTS

OUTBOARD DUCTS

FUSELAGE

$C_{n_\beta}$ ~
per deg

AIRCRAFT — VERTICAL TAIL

$C_{n_\beta}$ ~
per deg

MACH NUMBER

$C_L$

CONFIDENTIAL

D-181-960-009

AIRPLANE DIRECTIONAL STABILITY
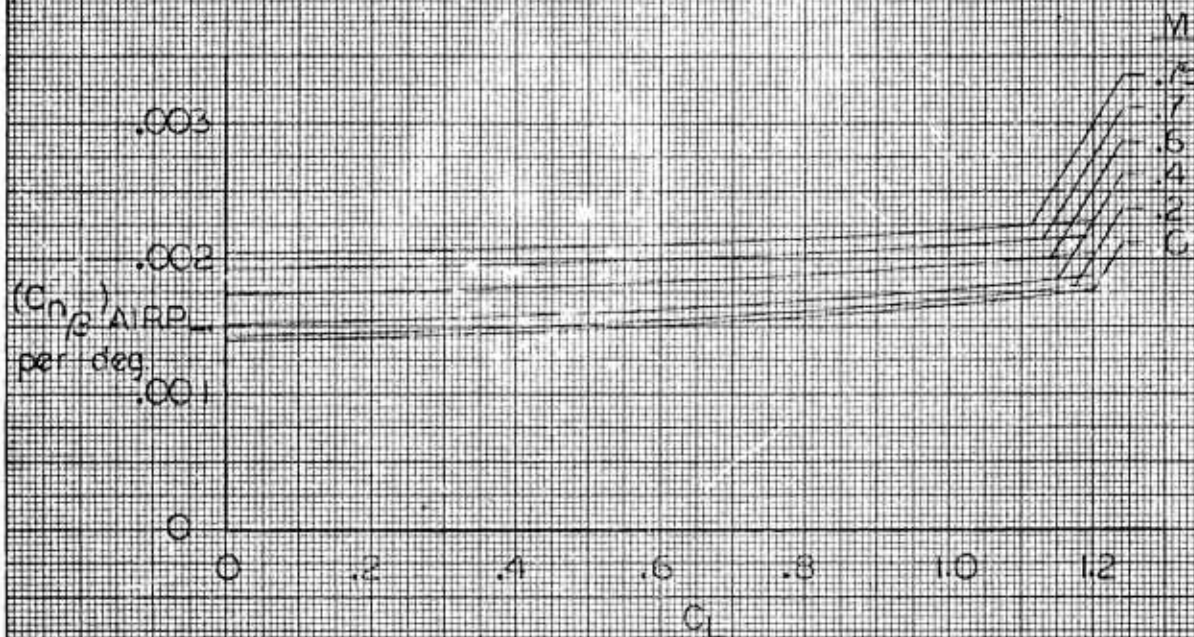
CONFIDENTIAL

Fig. No. 34

D-181-945-009

ROLLING STABILITY

CONTRIBUTION OF COMPONENTS
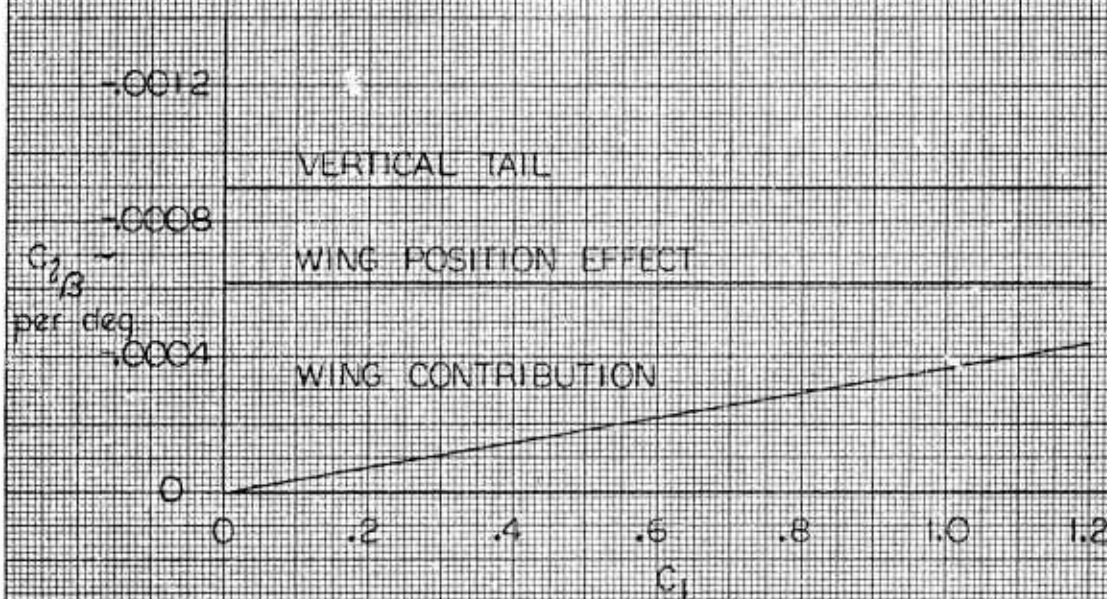
$C_{l_\beta}$ ~ per deg

VERTICAL TAIL

WING POSITION EFFECT

WING CONTRIBUTION

CONFIDENTIAL

Fig. No. 35

D-181-900-009

ROLLING STABILITY OF AIRPLANE
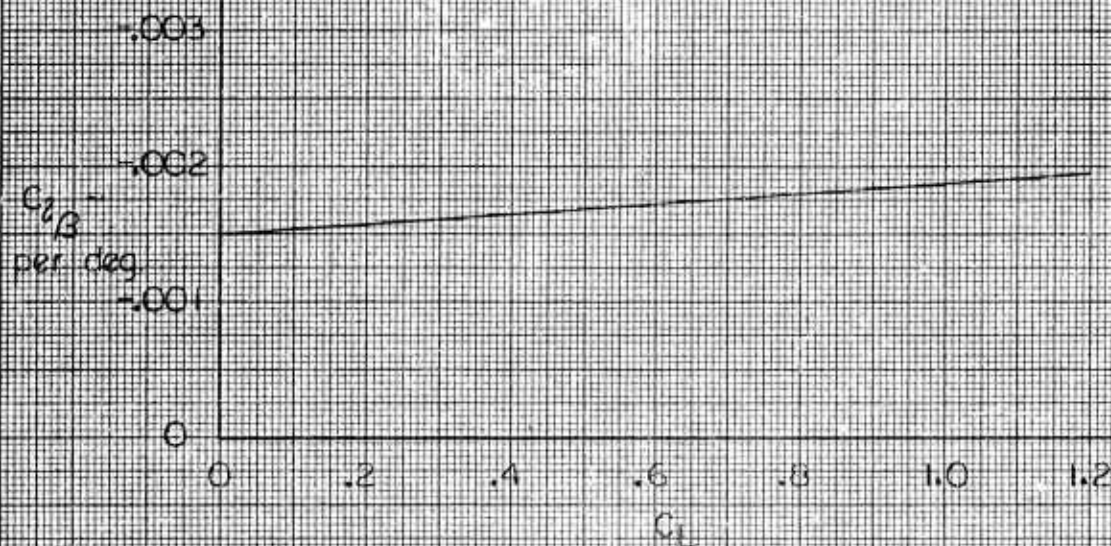
Fig. No. 36

D-181-960-009

DAMPING IN ROLL FOR WING
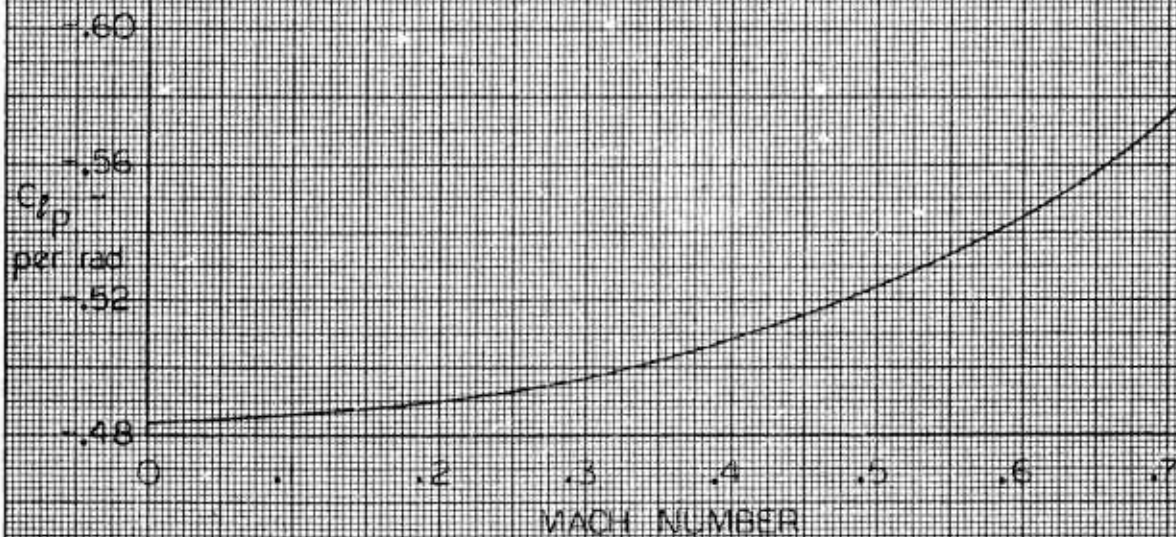
Fig. No. 39

D-181-960-009

VERTICAL TAIL DAMPING IN YAW
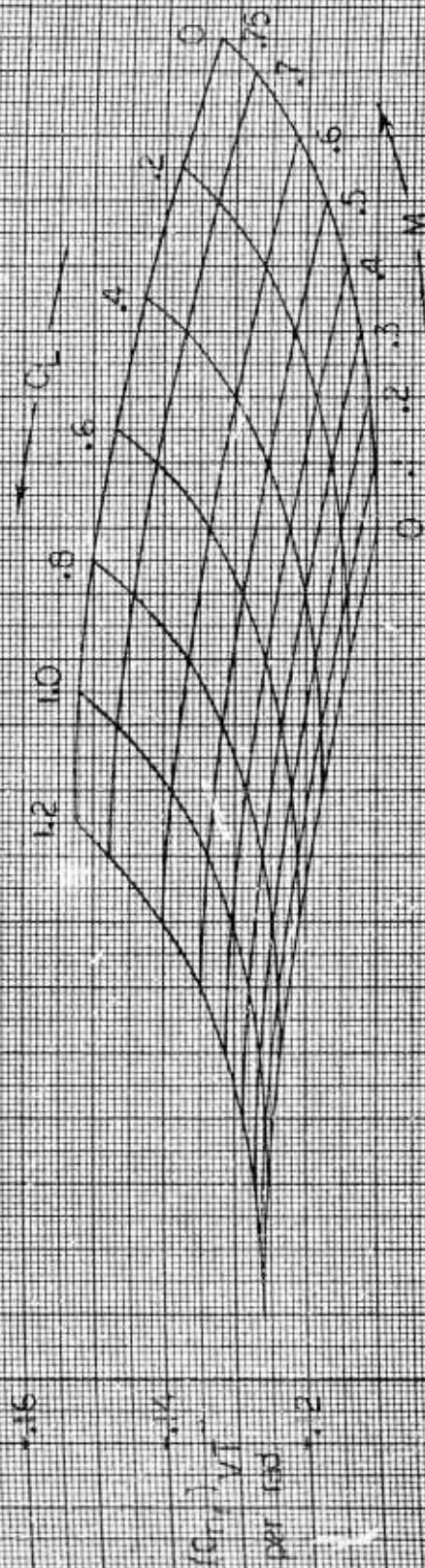
Fig. No. 38



D-181-960-009

WING DAMPING IN YAW

FIG. No. 39



D-181-960-009

AIRPLANE DAMPING IN YAW
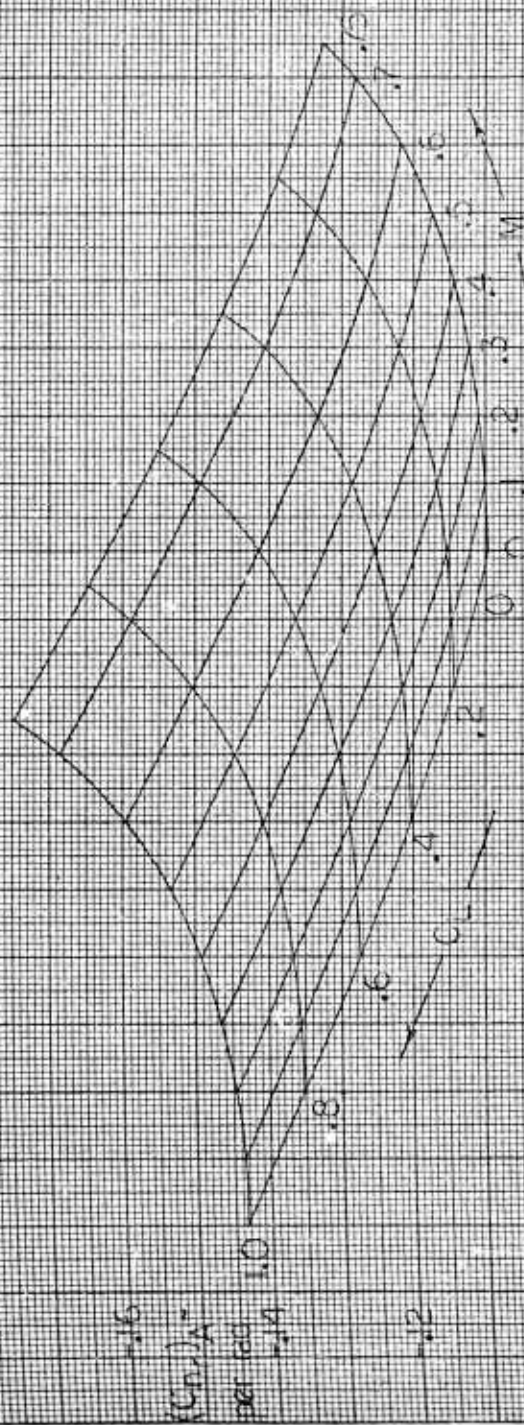
CONFIDENTIAL

D-181-960-009

HORIZONTAL TAIL

DAMPING IN PITCH

Fig. No. 40

$(C_{mq})_{HT}$ per rad

MACH NUMBER
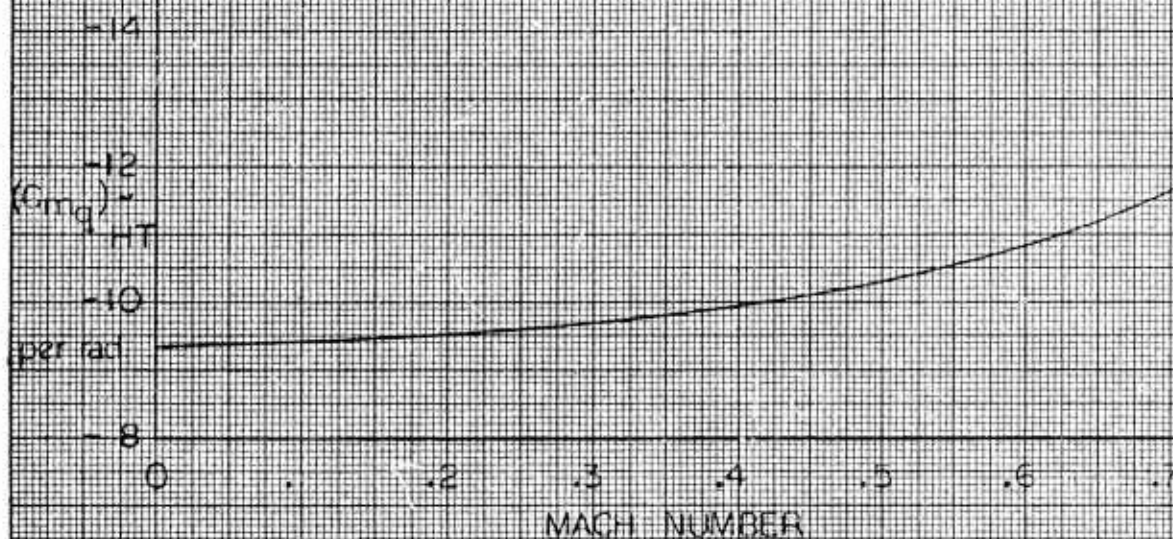
CONFIDENTIAL

Fig. No. 41



AIRPLANE ROLLING MOMENT DUE TO YAWING ANGULAR VELOCITY

D-181-950-009
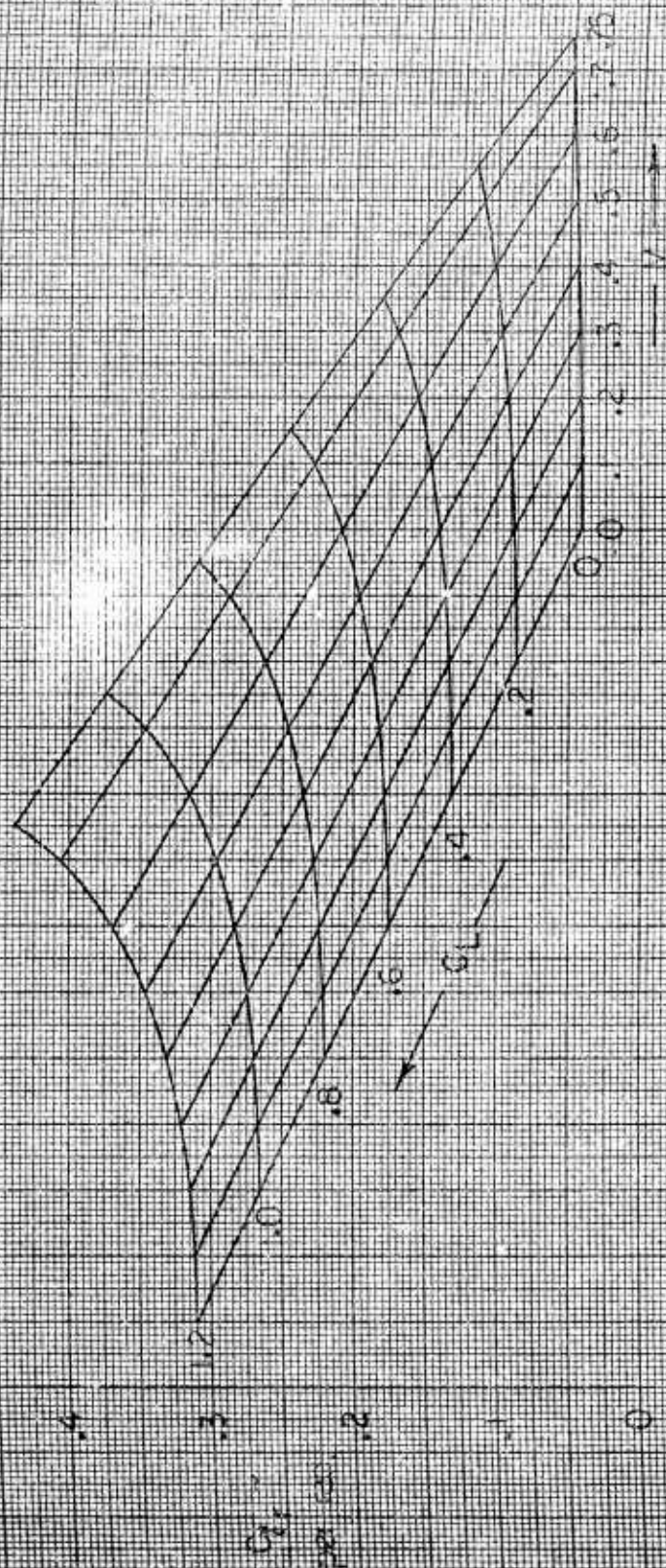
Fig. No. 42



D-181-940-009

AIRPLANE YAWING MOMENT DUE TO ROLLING ANGULAR VELOCITY

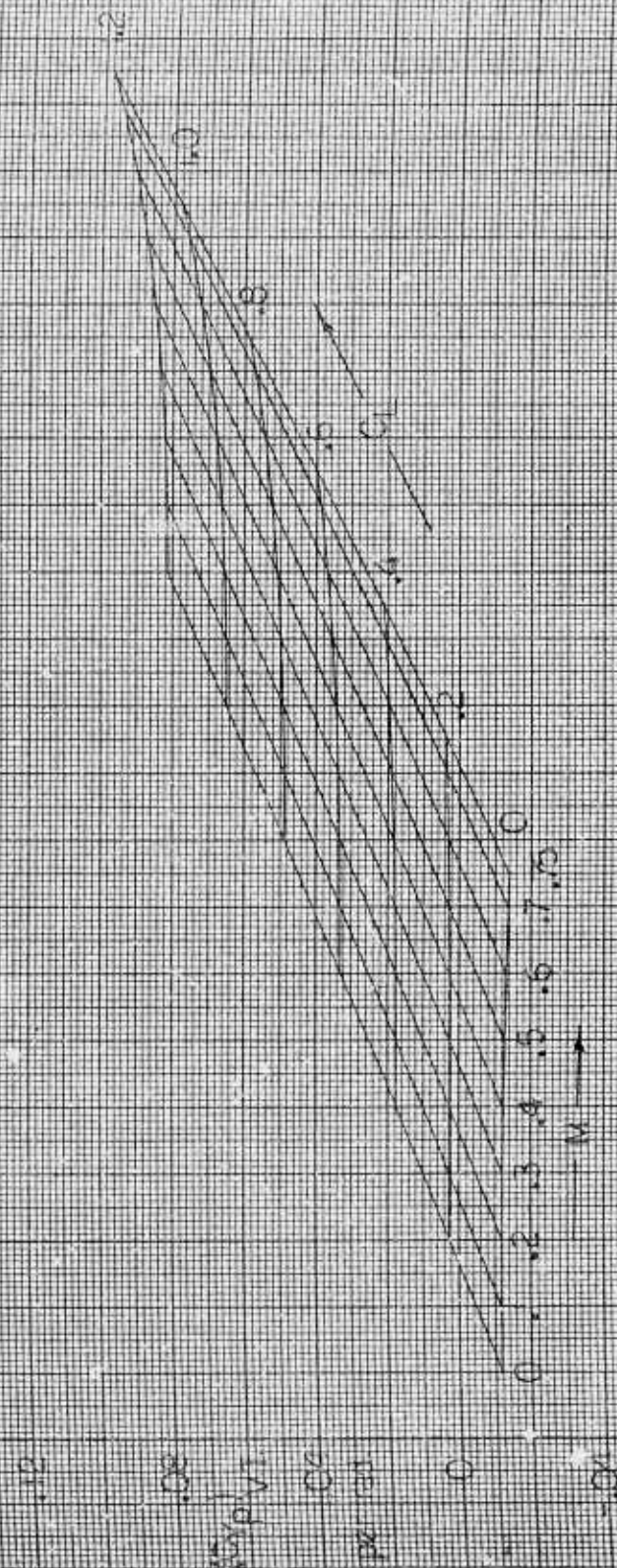FIG. No. 43

D-181-945-005

SIDE FORCE DUE TO ROLLING ANGULAR VELOCITY FOR VERTICAL TAIL

Fig. No. 4



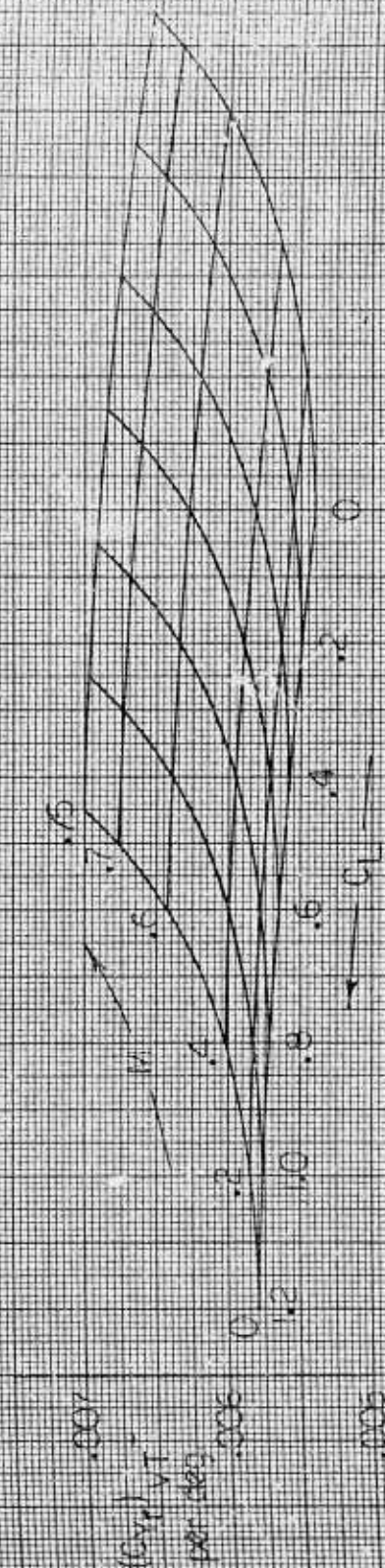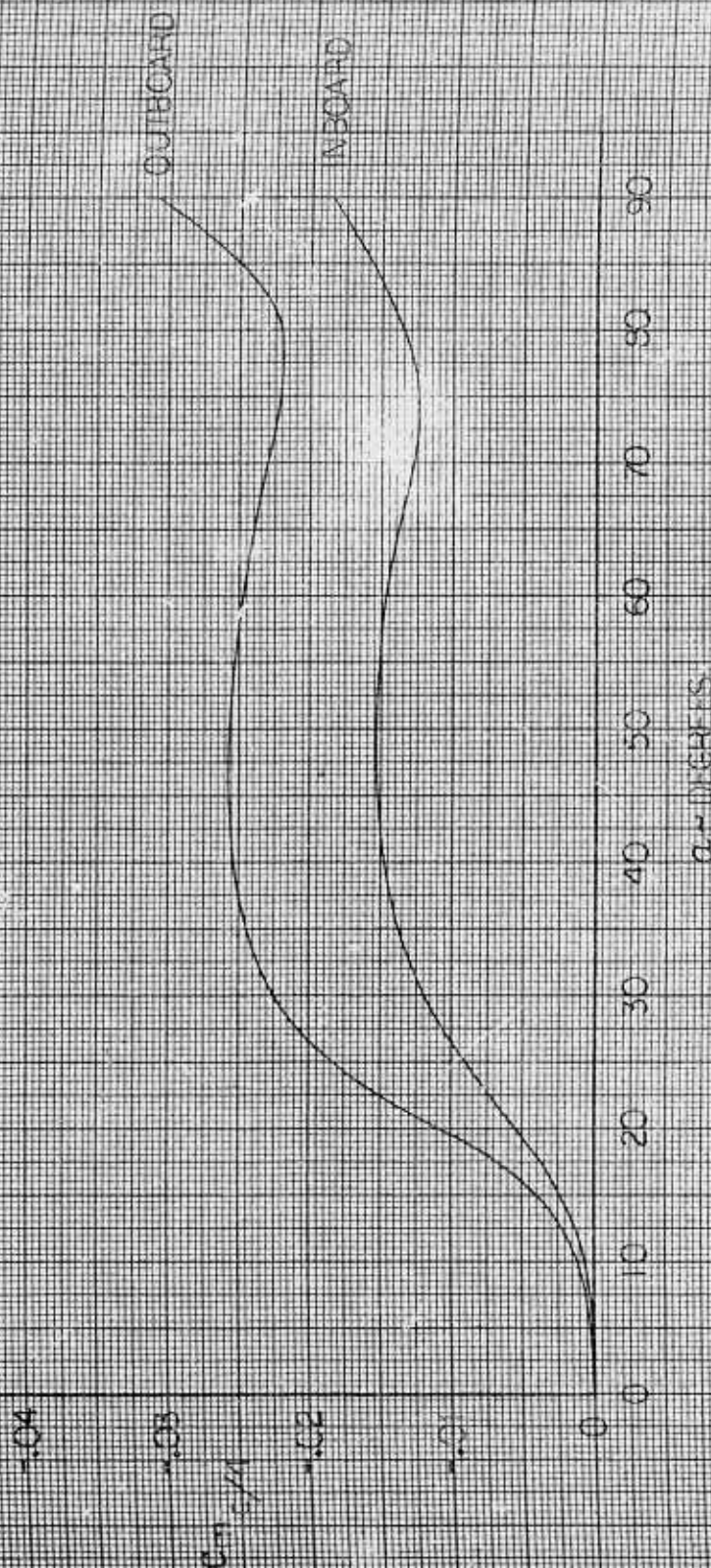SIDE FORCE DUE TO YAWING ANGULAR VELOCITY FOR VERTICAL TAIL

D-181-960-009

POWER OFF PITCHING MOMENT COEFFICIENT
PER DUCT

D-181-960-009    ALLISON 550 ENGINES

$S_{REF} = 1240 FT^2$

FLAPS CLOSED

MOMENT ABOUT 1/4 CHORD DUCT

OUTBOARD

INBOARD

$C_m = C/A$

$\alpha \sim DEGREES$

Fig. No. 45

CONFIDENTIAL

FIG. No. 46



POWER-OFF LIFT COEFFICIENT
PER DUCT

D-181-960-009    ALLISON 550 ENGINES

$S_{REF} = 1240$ FT.$^2$
FLAPS CLOSED

$C_L$

$\alpha \sim$ DEGREES

OUTBOARD

INBOARD

POWER-OFF DRAG COEFFICIENT
PER DUCT
ALLISON 550 ENGINES
$S_{REF} = 1240$ FT$^2$
FLAPS CLOSED

D-181-960-009

OUTBOARD

INBOARD

$\alpha \sim$ DEGREES

Fig. No. 48

D-181-945-005
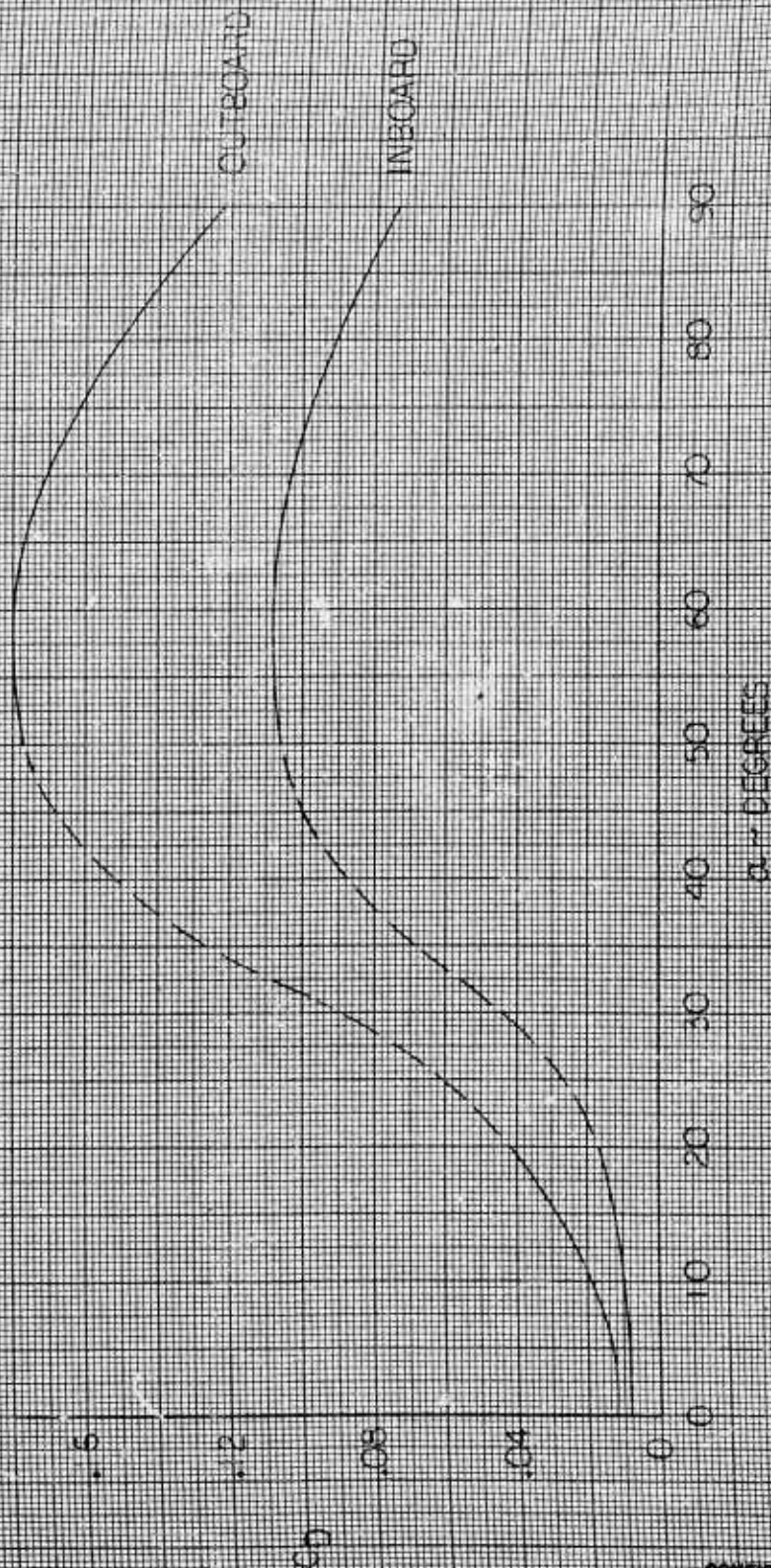
EFFECT OF AILERON SIZE IN TRIMMING AIRPLANE ATTITUDE
TO ZERO BANK ANGLE WITH INBOARD ENGINE OUT

W.T. = 72,100 lbs.
Hovering Attitude

(1) Inboard Engine Out

30% (b/2)

95% (b/2)

95% (b/2)

—————— 50% c  Ailerons
— — — —  25% c  Ailerons

Roll Trim Out Speeds

| | V | | |
|---|---|---|---|
| 95% (b/2) | 50% c | 75 Ft/Sec. | |
| | 25% c | 92 " | |
| 30% (b/2) | 50% c | 122 " | |
| | 25% c | 151 " | |

Reaction Control, φ = 7.5°/Sec²
δₐ = 20°

Rolling Moment, Pound Feet x 10⁻³

280  240  200  160  120  80

0   20   40   60   80   100   120   140   160   180   200

Velocity, Ft./Sec.